University of Reading

The role of local orography on the development of a severe rainfall event over western Peninsular Malaysia: a case study

Article

Accepted Version

Mohd Nor, M. F. F., Holloway, C. E. ORCID: https://orcid.org/0000-0001-9903-8989 and Inness, P. M. ORCID: https://orcid.org/0009-0005-5795-6841 (2020) The role of local orography on the development of a severe rainfall event over western Peninsular Malaysia: a case study. Monthly Weather Review, 148 (5). pp. 2191-2209. ISSN 1520-0493 doi: 10.1175/MWR-D-18-0413.1 Available at https://centaur.reading.ac.uk/89721/

It is advisable to refer to the publisher's version if you intend to cite from the work. See Guidance on citing.

To link to this article DOI: http://dx.doi.org/10.1175/MWR-D-18-0413.1

Publisher: American Meteorological Society

All outputs in CentAUR are protected by Intellectual Property Rights law, including copyright law. Copyright and IPR is retained by the creators or other copyright holders. Terms and conditions for use of this material are defined in

the End User Agreement.

www.reading.ac.uk/centaur

CentAUR

Central Archive at the University of Reading

Reading's research outputs online

LaTeX File (.tex, .sty, .cls, .bst, .bib)

Click here to access/download;LaTeX File (.tex, .sty, .cls, .bst, .bib);amspaper.tex

The Role of Local Orography on the Development of a Severe Rainfall Event over Western Peninsular Malaysia: A case study.

Mohd Fadzil Firdzaus Mohd Nor *

Institute of Ocean and Earth Sciences, University of Malaya, Kuala Lumpur, Malaysia

Christopher E. Holloway and Peter M. Inness

Department of Meteorology, University of Reading, Reading, United Kingdom

Corresponding author address: Mohd Fadzil Firdzaus Mohd Nor, Institute of Ocean and Earth Sciences, University of Malaya, 50603 Kuala Lumpur, Malaysia.

E-mail: fadzil.mnor@um.edu.my

ABSTRACT

Severe rainfall events are common in western Peninsular Malaysia. They are usually short and intense, and occasionally cause flash floods and landslides. Forecasting these local events is difficult and understanding the mechanisms of the rainfall events is vital for the advancement of tropical weather forecasting. This study investigates the mechanisms responsible for a local heavy rainfall event on 2 May 2012 that caused flash floods and landslides using both observations and simulations with the limited-area high-resolution UK Met Office Unified Model (MetUM). Results suggest that previous day rainfalls over Peninsular Malaysia and Sumatra Island influenced the development of overnight rainfall over the Strait of Malacca by low-level flow convergence. Afternoon convection over the Titiwangsa mountains over Peninsular Malaysia then induced rainfall development and the combination of these two events influenced the development of severe convective storm over western Peninsular Malaysia. Additionally, anomalously strong low-level northwesterlies also contributed to this event. Sensitivity studies were carried out to investigate the influence of the local orography on this event. Flattened Peninsular Malaysia orography causes a lack of rainfall over the central part of Peninsular Malaysia and Sumatra Island and produces a weaker overnight rainfall over the Strait of Malacca. By removing Sumatra Island in the final experiment, the western and inland parts of Peninsular Malaysia would receive more rainfall, as this region is more influenced by the westerly wind from the Indian Ocean. These results suggest the importance of the interaction between land masses, orography, low-level flow and the diurnal cycle on the development of heavy rainfall events.

1. Introduction

Western Peninsular Malaysia is the most densely populated area of Peninsular Malaysia with at least 65% of the Malaysian population. The Strait of Malacca is adjacent to the western coast of Peninsular Malaysia and the eastern coast of Sumatra Island and is one of the busiest sea traffic lanes in the world. This area has interesting weather patterns mostly affected by the interaction between the atmosphere and local orography (Figure 1). In Peninsular Malaysia, severe weather events such as flash floods, landslides, and strong wind storms are the main meteorological threats affecting the socioeconomic factors of the people in this region. A better understanding of the processes affecting such events is essential for improving forecasts and minimizing loss.

Localized convective rainstorms usually develop from thermal convection aided by warm surface temperature and surface land heating due to solar insolation. Local orography, local weather circulations such as land-sea breezes, and large-scale weather patterns such as monsoons will influence and modify local weather. For cases in Peninsular Malaysia and nearby islands, the following mechanisms involved in the development of localized severe convection have been discussed in previous studies:

1) the interaction between the gravity waves produced by the orography and the gravity waves produced by the advancing westerly sea breeze front over the west coast (Joseph et al. 2008);

2) the daytime sea breeze being reinforced by the valley breeze circulation, enhancing convergence over the mountainous region (Qian 2008);

3) the sea breeze collision between easterly and westerly sea breeze fronts enhancing convection inland (Joseph et al. 2008; Qian 2008);

4) the interaction between the lee waves over the mountainous area and the westerly sea breeze front which is common over northwest Peninsular Malaysia (Sow et al. 2011);

5) the gap wind associated with a strong wind from the east passing through the mountains pushing the inland convection toward the west (Sow et al. 2011).

These studies show the critical role of local orography and coastal circulations in developing and modifying the weather in this region.

Fujita et al. (2010) argue that colder and denser low-level air flow ("cold flow", as compared to surrounding air temperature) originates from the inland region of both Sumatra and Peninsular Malaysia usually formed from previous evening rainfall, is essential for convective activity over the Strait of Malacca. The study found that after evening rainfalls at approximately 19:00 Malaysian Standard Time (MST, +08 UTC), in both Sumatra and Peninsular Malaysia there were cold flows from both regions flowing toward the Strait of Malacca with a speed of 5-6 m s^{-1} and converging in the middle of the strait at approximately 01:00 MST. The peak time of the maximum rainfall recorded over the strait was 05:00 MST. Fujita et al. (2010) also revealed that the width of the Strait of Malacca (approximately 360 km between the mountain peaks of Sumatra and Peninsular Malaysia) affected the timing and location of the rainfall over the strait. Furthermore, in their model experiment, when the gap between Sumatra and Peninsular Malaysia was widened orthogonally by an increment of approximately 100 km, the average peak time of maximum rainfall in the middle of the strait are varied. For the 100 km-wide experiment, it was around 07:00 MST and for the 200 km-wide experiment, the peak time of maximum rainfall in the middle of the strait was around 10:00 MST. The 300 km-wide experiment showed that the peak time was 13:00 MST. In the wider strait experiments (200 and 300 km experiments), the two cold flows from both regions did not manage to converge before the rainfall as it rained before the two cold flows merged and weaker convection was observed. Therefore, a wider strait caused a later and weaker rainfall.

Simulating precipitation over the tropics is subject to significant errors in accuracy in term of location and time and as such remains open to improvement. Parameterized convection schemes

used in coarse resolution models generally show unrealistic results, such as an overestimated rainfall area or rainfall events that occur too early in the day as compared to observations (e.g. Birch et al. 2016). Higher resolution models improve the representation of orography and they generally have better mesoscale circulation and rainfall simulation, most likely because the models simulate convective rainfall explicitly (Birch et al. 2016). While precipitation processes are complicated, the physical mechanisms involved can be well represented by explicit convection simulation. For example, a study from Golding (1993) showed that the 3 km MetUM model was able to capture topographically forced thunderstorm genesis and the internal structure of thunderstorms including the trade level inversion and mid-level rotation. Gravity waves are also generally well represented by higher resolution models as in the 4 km MetUM Unified Model run in Love et al. (2011) which simulated convection propagation over the Sumatra region. This study found that gravity waves triggered offshore convection in the explicit convection model, but the insensitivity of the convective parameterization in the lower resolution 40 km model was unable to correctly trigger convection as the gravity waves parsed.

To investigate the development of heavy rainfall over western Peninsular Malaysia, a case study on 2 May 2012 was selected in which the Klang Valley (circled in red in Figure 1) experienced severe convective storms that caused flash floods. This event disrupted everyday activities and damaged property. The maximum hourly rainfall rate was 22 mm hr^{-1} and a total of 53.2 mm of rain was observed within 5 hours at one of the nearest stations (Figure 2a and b). The maximum rainfall occurred at 16:00 MST, weakened an hour later, and stopped at 18:00 MST. The heaviest rainfall occurred mostly over the central west coast of the peninsula.

This event occured during the inter-monsoon period (April-May and September-October, for Malaysia). During this period, the Inter-tropical Convergence Zone climatologically occurs near the equatorial region and increases local convective activity. The inter-monsoon period is also the

time when western Peninsular Malaysia receives a higher total of rainfall, especially from afternoon rainfall, compared to the other seasons (MetMalaysia 2016). This is also shown in Figure 2c, where climatological monthly mean of precipitation from Topical Rainfall Measurement Mission (TRMM) is given for three regions of western and inland Peninsular Malaysia (red boxes in Figure 4). The total daily rain amount for this event in the west coast was 35.5 mm day^{-1} which is higher than the 90th percentile of 20.3 mm day^{-1} (calculated by considering days averaging $\geq$ 1 mm day^{-1}). Thus, this day is considered to be a heavy rainfall day. On 2 May 2012, Sumatra and Peninsular Malaysia also experienced anomalously strong westerly winds from the Indian Ocean and northwesterly winds over the Strait of Malacca (Figure 3). This event did not occur during a Madden-Julian Oscillation (MJO) active phase; the Real-Time Multi-variate MJO index (Wheeler and Hendon 2004) was less than 1 (weak MJO) between 25 April and 17 May 2012 (Bureau of Meteorology Australia 2015). Additionally, the event also occurred during a neutral phase of El Niño-Southern Oscillation (ENSO).

It was hypothesized that the evening rainfall over Peninsular Malaysia and Sumatra island on the day before the event helped in generating rainfall over the Strait of Malacca overnight. Additionally, the morning rainfall over the Strait of Malacca helped to induce the regeneration of convective activity over the west coast of Peninsular Malaysia after merging with the rainfall cluster over the Titiwangsa Mountains. Furthermore, stronger westerly and northwesterly winds from the Indian Ocean helped enhance the development of the heavy convective rainfall. This study investigated the mechanisms involved in the development of the rainfall event using the high-resolution MetUM. While other studies have focused on modifying thermodynamic features (Fujita et al. 2010; Sow et al. 2011) and moving land masses (Fujita et al. 2010) to study the convective rainfall mechanism in this specific region, this study will evaluate the importance of orography and land versus sea regions on rainfall development by flattening mountains and removing the island of Sumatra.

2. Data and Methodology

a. Data

This study used the 3-hourly data from the Tropical Rainfall Mission Measurement (TRMM, 3B42 Version 7) which has $0.25^\circ \times 0.25^\circ$ resolution where all values are in mm hr^{-1} (Huffman and Bolvin 2007). The 3B42 algorithm produces an adjusted rainfall rate which combines other precipitation estimates from the TRMM Microwave Imager (TMI), Special Sensor Microwave Imager (SSMI), Advanced Microwave Scanning Radiometer for Earth Observing System (AMSR-E), Special Sensor Microwave Imager/Sounder (SSMIS), Microwave Humidity Sounder (MHS), Advanced Microwave Sounding Unit (AMSU), and microwave-adjusted merged geo-infrared (IR) (Huffman and Bolvin 2007).

An hourly rainfall dataset of rain gauge measurements from Petaling Jaya station of the Malaysian Meteorological Department (MetMalaysia) was used as a reference. Radar images from the Malaysian Meteorological Department (MetMalaysia) from 00:00 MST 2 May 2012 - 20:00 MST 2 May 2012 were used to detect the location and time of the rainfall. According to Kamaruzaman et al. (2012), MetMalaysia uses the Z-R relationship method of Marshall-Palmer (Marshall and Palmer 1948; Battan 1973) to convert the reflectivity (Z, in mm^{-6} m^3) to rain rate (R, in mm hr^{-1}) using the $Z=200R^{1.6}$ formula. At the time of this study conducted, MetMalaysia used an optimization method (regression technique) to find the best correlation and minimize the error between Z and R since there was no disdrometer instrument to measure raindrop size distribution in Malaysia (Kamaruzaman et al. 2012).

Other data mentioned or used include the GES DISC Multi-year Monthly Mean Product from AIRS Monthly Retrieval Data AIRX3STM_V006 which can be found on the Giovanni website (NASA 2019) for surface air temperature anomalies, and the NCEP/NCAR Reanalysis Project

from the National Oceanic and Atmospheric Administration (NOAA) PSD, Boulder, Colorado, USA, taken from their website for wind anomalies (NOAA 2019). The AIRS data were available from September 2009 until September 2016 at 1° spatial resolution. The data were Level 3 monthly gridded standard retrieval product using the AIRS infrared spectrometer, a visible imager, and two microwave radiometers which were Advanced Microwave Sounding Unit (AMSU) without the Humidity Sounder for Brazil (HSB). The NCEP/NCAR Reanalysis data was on a 2.5° × 2.5° global grid, with 17 pressure levels.

b. Model Setup

The model setup in this study was similar to Holloway et al. (2013). A limited area model of MetUM version 7.5 was used with two domains (see Figure 4), with a 12 km grid spacing for the outer domain and a 1.5 km grid spacing for the inner domain. The model used the New Dynamics dynamical core based on semi-implicit semi-Lagrangian and non-hydrostatic Euler equations (Davies et al. 2005). The 12-km model (154 × 172 grid) used a 0.11° × 0.11° resolution while the 1.5-km model (666 × 814 grid) used a 0.0135° × 0.0135° resolution. There were 38 vertical levels in the 12-km model and 70 vertical levels in the 1.5-km model. The 12-km model had a maximum height of 37 km, and the 1.5-km model had a maximum height of 40 km. The 12-km model used a parameterized convection scheme and the lateral boundary conditions (LBCs) were updated from ECMWF analyses every 6 hours, using a rim of 8 model grid points around the domain. The 1.5-km model lateral boundary condition were updated from the 12-km model output every 30 minutes using an 8 model grid point rim width. The rim is the place at which the prognostic fields were blended linearly between the outer analysis or driving model data and the inner model domain. The model setup was one-way nested.

The model physics in the 12-km model used a modified Gregory-Rowntree convective parameterization with 30-min convective available potential energy (CAPE) relaxation time scale, thus using CAPE as the basis of its closure (Gregory and Rowntree 1990). The 12-km model also used a standard boundary layer scheme for vertical subgrid mixing (Lock et al. 2000) without horizontal subgrid mixing. This model also used single-moment mixed-phase microphysics with two components which are liquid water and ice/snow (Wilson and Ballard 1999). The model physics in the 1.5 km model was the same as in the 4-km 3Dsmag model in Holloway et al. (2013) but was reduced to a 1.5 km grid. The same CAPE-limited version of the convective parameterization was used, and over 99% of the rainfall was generated explicitly (Lean et al. 2008). Based on previous literature, convective parameterization in the 1.5 km model helped with the model's stability, but the parameterization should not have had much of an effect on deep convection and resulting circulations (Lean et al. 2008; Love et al. 2011; Holloway et al. 2012). The model used the Smagorinsky-type subgrid mixing in all three dimensions. No boundary layer scheme (as in the 12-km model) was used. The Smith cloud physics scheme (Smith 2014) was used in both 12-km and 1.5-km model simulations.

c. Methodology

Rainfall datasets from TRMM, gauges and radar images were used to detect the time and location of the rainfall event. The control (CTR) run was used to compare the model output to the observations and to analyze the development of this event in greater detail. Four sensitivity experiments tested the role of local orography and land versus sea coverage in the development of the event. The same model reconfiguration (to create the initial condition file) as in the CTR run was used with the exception that the orography and land-sea mask fields were modified in an ancillary file depending on the objective of the experiment. As the experiments were only run for the 1.5-km

model, all experiments used the same 12-km model LBC file as the CTR run. The experiments were run on the same model period as in the CTR run. The modifications of each experiment are represented in Figure 5.

The experiments modified the orography and land-sea mask as follows:

1. (**flatPM**) The orography of the peninsula and the closest small islands was flattened to sea level.

2. (**flatSI**) The orography of Sumatra Island and the closest small islands was flattened to sea level.

3. (**flatALL**) The orography of Peninsular Malaysia, Sumatra, and the surrounding small islands was flattened to sea level.

4. (**noSI**) Sumatra was removed; the orography of Sumatra was initially flattened to sea level, and the land-sea mask file was then adjusted by removing the land points (Sumatra and the surrounding small islands) and replacing them with ocean points.

In the **noSI** experiment, the land point value in the land-sea mask file was changed to sea value to represent the ocean and treated like an ocean. The roughness length and the surface latent heat flux were considered the same as the ocean and the sea surface temperature was interpolated from the nearest sea points.

To investigate the effects of orography modification on the rainfall amount, the peninsula was divided into three regions - northwestern, western and inland peninsula as well as the central strait (see Figure 4 in red) and the rainfall amounts for each region were calculated. This area division was a modified version of the one used in Suhaila and Jemain (2009) which is based on geographical division. The selection of the region over the strait (MS) was based on the majority of

rainfall that occurred in this case study. In all discussions hereafter, only 1.5-km model simulation results are discussed.

3. Results and Discussion

a. Observations

Besides the information presented in the final part of the introduction section, the rainfall event was also detected in radar images as shown in Figure 6 (top). A cluster of rainfall was observed over the Strait of Malacca, as well as parts of northwestern and west-central Peninsular Malaysia at 11:00 MST. By 12:00 MST, more rainfall clusters had spread across the western side of the peninsula and along the Titiwangsa Mountains (see Figure 1) and became intense by 13:00 MST. As the intensity of the rainfall increased over the western peninsula at 14:00 MST, the rainfall over the Strait of Malacca weakened. The rainfall over the western peninsula strengthened and spread to a larger area by 15:00 MST. It stayed on the west coast until 18:00 MST and had subsided at 20:00 MST (Figure 8a: C).

While it is common to have severe afternoon rainfalls during the intermonsoon period, observational data from the NASA's Atmospheric Infrared Sounder (AIRS) indicated that an anomalously cold area of near-surface air had developed from Sumatra Island which had then propagated eastward into the Strait of Malacca from early April until early May 2012 (not shown). There was also an anomalously strong westerly wind from the Indian Ocean and at the same time stronger northwesterly wind over the northern part of the Strait of Malacca, on 1 and 2 May 2012 (Figure 3). The Convective Available Potential Energy (CAPE) at the MetMalaysia's Sepang station revealed that the CAPE value on the evening of 1 May (20:00 MST) was 2361 J kg^{-1}, and on the morning of 2 May 08:00 MST was 1786 J kg^{-1} with the Convective Inhibition of -3.16 J kg^{-1} and -21.3 J

241 kg^{-1} respectively (University of Wyoming 2016). These conditions favored the development of a
242 severe rainstorm.

243 *b. Simulation : Control Run (CTR)*

244 The radar images (Figure 6a) showed the development of convective precipitation over western
245 Peninsular Malaysia at approximately 13:00 MST which intensified by 14:00 MST and 15:00
246 MST. As we have hypothesized earlier, the morning rainfall over the Strait of Malacca might
247 have helped to induce the development of convective activity over the west coast of Peninsular
248 Malaysia after merging with the rainfall cluster over the Titiwangsa Mountains. Although not
249 perfect in terms of location of the rainfall (Figure 6b), the model simulation reproduced most of
250 the ranfall event shown in the radar images. The main features, such as the rainfall over the strait
251 and along the Titiwangsa Mountains, are well represented. The model indicates more variability
252 in rainfall intensity over Peninsular Malaysia compared to the radar.

253 The 3-hourly mean precipitation from the TRMM (Figure 7) dataset demonstrates a realistic
254 comparison to the radar images (Figure 6a). Additionally, the TRMM dataset captured the rainfall
255 event in Peninsular Malaysia on the previous day (1 May) which was not available from the radar.
256 The model simulates the precipitation over the strait as in TRMM, although not perfectly. The
257 model also simulates other observed features such as rainfall events in the southeast (14:00 MST)
258 and the east coast of Peninsular Malaysia (17:00 MST).

259 The severe rainfall event in this simulation concentrated on the west coast at around 3°N to
260 4°N and the evolution of the rainfall event can be viewed in the time-longitude Hovmöller plot
261 in Figure 8a. On the day of the event (black horizontal dashed line), the rainfall over the strait
262 started around 05:00 MST on 2 May and propagateed eastward within 9 hours for about 100
263 km or at approximately 3 m s^{-1} (Figure 8a: A). It mostly dissipated mostly before reaching the

coast. The rainfall over the Titiwangsa Mountains (Figure 8a: B) started around 12:00 MST and within one hour propagated westward and eastward within one hour. Compared to TRMM in Figure 8b, there were rainfall events over both landmasses before the event, agreeing with the model (Figure 8a: E and 8b: Z). TRMM showed that there were rainfall events over the strait, but these did not propagate as seen in the model (Figure 8a: A and 8b: V). Similar events over both sides of the peninsula were in agreement between the model and TRMM (Figure 8a: C and D versus 8b: X and Y). The rainfall that developed over the Titiwangsa mountains was also captured in the model, similar to the TRMM (Figure 8a: B and 8b: W). The modeled westward-propagating rainfall cluster lasted longer and was weaker than the observed cluster (Figure 8a: C versus 8b: X). The modeled westward-propagating rainfall cluster later combined with the rainfall event over the coast at approximately 14:00 MST (Figure 8a: C) and remained over the west coast for a couple of hours. The modeled eastward-propagating rainfall cluster gradually subsided after almost 30 minutes. However, another rainfall cluster over the east coast (Figure 8a: D) developed and propagated eastward following the mean westerly wind. This figure indicated the rainfall event that occurred on the previous day in both Sumatra Island and Peninsular Malaysia (Figure 8a: E) could be one of the main factors that have contributed to the development of the severe event on 2 May in the Strait of Malacca.

The modeled mean wind circulation over 3°N to 4°N is shown in Figure 9 at 233-meter model (hybrid) level (which is 233 m for columns beginning at sea level). The colors represent wind speed, and the vectors represent the wind direction. Most of the time, the wind was stronger in the Strait of Malacca compared to the Indian Ocean (leftmost area) and the South China Sea (rightmost area). In the morning before the event (before the black dashed line), the winds over the Strait of Malacca were mostly northwesterly (Figure 9 A). The westerly winds were stronger and progressed eastward across the peninsula during the event (Figure 9 B). The northwesterly

winds were stronger over the peninsula before the rainfall event, on both 1 and 2 May (Figure 9 C). Although there were not enough days for analysis to make a robust determination, stronger northwesterly winds in the strait may have been one of the main factors in the development of the heavy rainfall over the western peninsula. The winds converged near the coast of the peninsula before the event (Figure 9 D) and the convergence could have been associated with the rainfall event. Stronger westerly winds before the event could also be a sign of stronger convection over the peninsula before the event occurred.

The diurnal cycle of land-sea breeze can also be seen in Figure 9. A stronger sea breeze occurred on both sides of the peninsula during the daytime. On the west coast of the peninsula, the sea breeze became stronger by 12:00 MST and moved further inland. On the east coast of the peninsula, the sea breeze began near the coast and gradually became stronger, starting off the coast and moving inland (Figure 9 E). Note that the sea breeze over the east coast of the peninsula in Figure 9(E) was constrained and not progressing further inland. It could have been affected by the severe rainfall event over the western peninsula and the stronger north-easterly winds coming from the strait and western peninsula. The land breeze (at night) on both the west and east coasts of the peninsula was weaker except in the early morning of 3 May.

c. Possible Mechanisms

Possible mechanisms leading to the event on 2 May can be hypothesized by examining the radar and the model in Figure 6. As seen in Figure 10, rainfall events from the afternoon of 1 May (Figure 10a: A and B)) might have influenced the development of the rainfall over the Strait of Malacca and saturated the land especially over the west coast of the peninsula to cause flooding on the next day. The rain intensified by 10:00 MST (Figure 10b: C), with the incoming northwesterly winds assisting the development of convection by increasing low level convergence

and the lifting of boundary layer parcels over the strait. In the early afternoon, convective activity was also observed over the Titiwangsa Mountains (Figure 10c). Later, these two rainfall clusters from the strait and Titiwangsa mountains merged over the western peninsula (red arrows in Figure 10c), influencing the development of convection over the central west of Peninsular Malaysia (Figure 10d: D) and produced rainfall. The Titiwangsa mountains blocked the rainfall cluster, and the rainfall cluster which remained on the west coast despite the incoming northwesterly wind. The local orography also helped to shape the direction of the wind. The westerly winds from the Indian Ocean were deflected towards the Strait of Malacca by Sumatra Island in the north, and the Titiwangsa Mountains in Peninsular Malaysia which kept the wind in a northwesterly direction until it changed to westerly at the southern Peninsular Malaysia. The northwesterly wind also influenced the convection over the Titiwangsa mountains which developed early at noon and moved or redeveloped on the east coast.

Near-surface temperature and specific humidity were used to investigate the possible contribution of the moisture from the previous-day rainfall to the development of the morning rainfall over the Strait of Malacca (Figure 11). Figure 11a shows the movement of anomalously cold near-surface temperature (blue shades) toward the strait. Both flows (density current along with land breezes) from Sumatra and the peninsula started moving slowly toward the strait around 23:00 MST and merged at the center of the strait. The moisture from previous rainfall was also transported toward the strait as shown in Figure 11b (red arrows). Higher moisture propagated slowly toward the strait from both land masses commenced at 21:00 MST and clustered at the center of the strait early on the morning of 2 May. Thus, the combination of colder air and moist air flows from both land masses favored the development of convective rainfall over the Strait of Malacca by providing additional moisture and low-level lift to the atmosphere. The converging flows can also be viewed in Figure 12. By 04:00 MST, there was a sign of converging wind flowing toward the

center of the strait. The converging winds were more pronounced where the flows from the land masses met the northwesterly wind flowing through the strait. This can also be cold outflow fronts moving from the coast regions of the land masses toward the center of the strait. The converging winds are co-located with, and plausibly contribute to the development of, scattered rainfall over the strait (dashed contours in Figure 12) as early as 05:00 MST. Converging winds continued to intensify through 08:00 MST and the rainfall clusters over the strait grew larger.

Sensitivity experiments were done to investigate how the local orography and Sumatra Island affected the rainfall development in this event, and these will be discussed in the next section.

d. The Role of Local Orography and Sumatra Island

1) The Role of the Titiwangsa Mountains

As we have discussed earlier, the **flatPM** experiment was conducted to investigate the role of the Titiwangsa Mountains (as in Figure 5, **flatPM**) and the result is shown in Figure 13e-h. The first noticeable difference is the lack of organized convection inland of the peninsula on the afternoon of 1 May (Figure 13e: A). A rainstorm cluster was observed in the morning of 2 May over the Strait of Malacca. The rainfall cluster over the Strait of Malacca was slightly tilted toward Peninsular Malaysia (Figure 13f: B), and it is associated with the westerly and northwesterly winds from the Indian Ocean. Without the Titiwangsa Mountains, these onshore winds are not restricted and are able to progress further inland onto the peninsula, causing the northern part of the rainfall cluster at the strait to be pushed toward the peninsula. Another difference is that in the early afternoon of 2 May (Figure 13g: C) there was no convection inland of the peninsula. However, there was still rainfall over the coast, due to the sea breeze interaction with the landmass. The event was less intense than in the control, and later that day the convection was pushed to the southeast by the prevailing northwesterly wind.

The Hovmöller Figure 14c shows the temporal evolution of rainfall clusters in the **flatPM** experiment. The rainfall over the western peninsula was weaker as seen in Figure 14c (A) and over time propagating eastward. The northwesterly wind influenced the rainfall cluster to propagate eastward and this is also the reason for the lower amount of rainfall on the west coast of Peninsular Malaysia as most of the rainfall cluster was pushed eastward (Figure 14d). The Hovmöller plot in Figure 14d shows the northwesterly winds observed over the Strait of Malacca the day before and in the early morning before the event. The low-level winds were mostly westerly on the afternoon of the event, and later the westerly wind advanced further inland (Figure 14d: B). Compared to the control, the daytime wind was weaker (blue shades) and the nighttime wind was stronger in the western peninsula when Titiwangsa mountains were removed. The northwesterly wind was slightly weaker in the strait before (Figure 14d: C) and slightly stronger during the day of the event (Figure 14d: B).

A weak easterly sea breeze observed on the east coast was associated with a weaker land-sea temperature gradient (reducing the land-sea breeze strength) as well as the absence of orographic convection inland of the peninsula. The plot in Figure 14d also shows some important wind-rainfall relationships in this experiment. For example, rainfall over the Strait of Malacca is associated with the converging low-level winds near the west coast of the peninsula.

2) The Role of the Barisan Mountains

The **flatSI** experiment was conducted to look at the role of the Barisan Mountains in Sumatra, and the result is shown in Figure 13i-l. In the late afternoon of 1 May (Figure 13i), there were rainfall events in both Peninsular Malaysia and Sumatra although there was weaker rainfall in Sumatra (Figure 13i: A). These rainstorms influenced the development of the rainfall event over the Strait of Malacca on the morning of 2 May (Figure 13j: B). Orographic convective rainfall was

also observed over the peninsula (Figure 13k: C). The rainfall that developed over the west coast of the peninsula was a combination of moist downdraft flow from the rainfall event over the Strait of Malacca and the developing sea breeze near the coast which merged with the orographic rainfall over the peninsula. The Titiwangsa Mountains had blocked the rainfall cluster from moving eastward for a couple of hours despite the prevailing northwesterly wind (Figure 13l).

The rainfall evolution in the **flatSI** experiment is shown as a Hovmöller plot in Figure 14e. The Hovmöller figure revealed that rainfall over the west coast of the peninsula occurred slightly earlier offshore than in the control run (around 1150 LT, Figure 14e: D) and propagated inland. The rainfall mechanism on the peninsula is the same as the one in the control run. Unlike the control run, there was less rainfall over Sumatra the day before, and rainfall from Sumatra started from the east coast and propagated eastward toward the strait (Figure 14e: E).

The Hovmöller plot of the lower level wind (Figure 14f) shows that the absence of the Barisan Mountains in Sumatra allows the westerly wind from the Indian Ocean to advance inland (Figure 14f: F). The wind over the strait on 1 May and early 2 May is weaker than in the control run. The wind over the strait (near to the west coast of the peninsula) was northerly before and during the event. The absence of Sumatra Island means there is no longer a narrow valley in between the island and the peninsula and could be the reason for the weaker wind over the strait (Figure 14f: G). On both days, the sea breeze over the east coast of Sumatra was generally weak.

3) The Role of both the Titiwangsa and Barisan Mountains

The **flatALL** experiment investigates the effect of high altitude orography on the rainfall pattern over the region. The flat landmasses caused weaker inland rainfall on 1 May (Figure 13m: A). These rainfall events (1 May afternoon) were, however, still influencing the development of the rainfall over the Strait of Malacca (Figure 13n). However, the rainfall cluster over the strait was

concentrated in the center of the strait, unlike in the control run. No orographic convective rainfall is present over the peninsula and Sumatra (Figure 13o). However, the rainfall over the strait still influenced the rainfall development on the northern part of the peninsula, and there was still rainfall occurring over the west coast in the afternoon (Figure 13p), mostly due to the interaction between the westerly wind, sea breeze and surface friction. Rainfall events were observed across the western coast at approximately 15:00 MST and dissipated as they move eastward following the northwesterly wind (not shown).

The rainfall evolution shown in Figure 14g indicated less rainfall on 1 May (Figure 14g: H), more rainfall over the strait as the rainfall becomes concentrated in the center of the strait (Figure 14g: K), and less rainfall during the day of the event (Figure 14g: L). The rainfall that developed over the western coast dissipated early and did not propagate eastward to the east coast in contrast with the other experiments. There was also a rainfall event over the west coast throughout the night between 1 May and 2 May. In the Hovmöller plot of the low-level wind in Figure 14h, the absence of the mountains in both Sumatra and the peninsula caused the westerly wind to advance inland. The wind was also weakened over the strait (Figure 14h: M) due to the absence of a narrow valley surrounded by mountains as explained in the previous section. The winds were mostly westerly in the early morning before the event. Without the orography, the westerly wind advanced inland smoothly across the peninsula (Figure 14h: N). The sea-breeze on the day of the event over the peninsula was also weakened as the stronger westerlies dominated the area.

4) The Role of Sumatra Island

The role of Sumatra Island was examined by conducting the **noSI** experiment as shown in Figure 13q-t. Rainfall events occurred on the afternoon of the previous day (Figure 13q), mostly in the north and south of the peninsula. A few rainfall events had developed off the western coast by

late morning, and there was also some rainfall over the northwestern peninsula (Figure 13s). The lack of early morning rain over the ocean did not prevent the rainfall development over the west coast on the afternoon of 2 May (Figure 13s). There were also rainfall events over the Titiwangsa Mountains from the orographic convention which lead to heavy rainfall over western peninsula later in the afternoon of 2 May (Figure 13t). The rainfall evolution in Figure 14i shows a few ocean rainfall events and the rainfall over the peninsula on 2 May which occurred almost simultaneously across the peninsula. There was also an early morning rainfall event over the west coast (around 0250 LT) which lasted for more than 4 hours, and another rainfall event later that day (around 19:00 MST). These three rainfall events contributed to a large amount of the total daily rainfall on 2 May. Thus, without Sumatra Island, rainfall would have been more frequent over the west coast from the 1 May until 2 May.

The winds would have been consistently westerly in the absence of Sumatra Island (Figure 14j: P). Interestingly, the westerly wind near the strait before the event was also weaker than the corresponding wind in control run near the western coast of peninsula (Figure 14j: Q). This shows that the narrow valley created by the mountains of both Sumatra Island and Peninsular Malaysia are essential in creating stronger winds over the Strait of Malacca. The wind on the east coast and the South China Sea (103.5 $^{\circ}$ E - eastward) prior to and a few hours after the event was also stronger than in the control run. One possible reason for this is that, as the winds reach the southern tip of the Titiwangsa mountains, they are deflected toward the South China Sea. Thus, because of the open ocean on the west, the western Peninsula of Malaysia is exposed to the westerly wind from the Indian Ocean. The specific humidity over central western Peninsular Malaysia in this experiment is also higher and is at least 0.87 g kg^{-1} on average when compared to the control run (not shown). Therefore, it is plausible that there is more moisture transported from the west and

that this westerly wind with extra humidity enhanced convective activity and rainfall over the west of Peninsular Malaysia.

5) Comparison of Rainfall Amount

The rainfall amount on the north-west, central west, inland and central Strait of Malacca regions (NWC, WC, IL, and MS respectively) from these experiments can be viewed in Figure 15. The total rainfall on 2 May (event day) in the CTR experiment shows a higher amount compared to the **flatPM** experiment in all four regions. The differences illustrate the importance of the Titiwangsa mountains in maintaining the rainfall cluster to the west. The rainfall total in the CTR run is higher in the WC and IL regions in the **flatSI** experiment although not in the NWC region. In the **flatALL** experiment, the NWC and WC received more rainfall than in CTR on 2 May, since more rainfall occurred in the coastal area rather than inland, as is further shown by the lower rainfall total in IL (compared to CTR). The total rainfall in the **NoSI** experiment was generally higher in all regions as compared to CTR on the 2 May, with the same reasons discussed earlier.

Most of the rainfall in the central area of the Strait of Malacca occurred on 2 May (Figure 15d). Larger rainfall amount in this region in the **flatALL** experiment can be explained by the inability of the rainfall cluster to merged together due to the absence of mountains in both Sumatra Island and Peninsular Malaysia. The mountains controlled the air circulation, flow and shape of the rainfall to almost a squall-line shape in this case study. Without these mountains, rainfall would mostly be concentrated in the center of the strait. In the **NoSI** experiment, the rainfall wass concentrated more on the land mass (peninsula) rather than the ocean as Sumatra Island was removed.

These experiments affected each region differently, but four common results were found:

1. removing the orography over Peninsular Malaysia reduced the rainfall in all three regions,

2. rainfall over the Strait of Malacca still occurred regardless of the height of the orography of both Sumatra and the peninsula,

3. both of the high mountain ranges in Sumatra and Peninsular Malaysia created a narrow valley that is responsible for creating a stronger wind over the Strait of Malacca, and

4. removing Sumatra Island caused more rainfall over the western peninsula. The higher total rainfall in the **NoSI** experiment was also attributed to the frequent rainfall events on 2 May which occurred during the early morning, mid-morning and evening.

4. Conclusion

This study investigated the role of orography in the development of a severe rainfall event in the Klang Valley region, Peninsular Malaysia on 2 May 2012. During the day itself, there were stronger westerly winds observed over the northern Strait of Malacca, with an anomalously cold near-surface air over Sumatra Island that moved eastward in late April and early May 2012. A case study was simulated using a limited-area setup of the high-resolution MetUM. The 1.5-km model realistically represented the rainfall event but slightly underestimated its intensity and had minor location errors. The 1.5-km model was able to represent the rainfall on 1 May over Peninsular Malaysia and Sumatra Island and the rainfall over the Strait of Malacca on the morning of 2 May. The model also reproduced the rainfall over the Titiwangsa Mountains of Peninsular Malaysia on 2 May.

Four sensitivity experiments were conducted to investigate the role of orography and land versus sea coverage on the development of the rainfall in this region. In the **flatPM** experiment, Peninsular Malaysia received less rainfall on 2 May compared to the CTR, as the absence of the Titiwangsa Mountains did not favor inland rainfall. Another reason for less rainfall in the western

peninsula was because the northwesterly wind had pushed the rainfall cluster eastward with no mountains blocking it. On 1 May, the convection over the Strait of Malacca existed because of the influence of rainfall on Sumatra Island and the small-scale rainfall over western Peninsular Malaysia. However, the rainfall intensity over the Strait of Malacca was weaker than in the CTR.

The **flatSI** experiment caused the rainfall over Sumatra Island on 1 May to be reduced significantly, but the rainfall over the peninsula was almost the same as in the CTR, including the rainfall over the Titiwangsa Mountains. This caused the rainfall activity in the Strait of Malacca to be less intense on the morning of 2 May. The combination of the rainfall event over the strait and the rainfall event over the Titiwangsa Mountains enhanced the severe rainfall event over western Peninsular Malaysia on 2 May. However, the rainfall was less than in the CTR over the west coast and inland.

When the orography of Sumatra Island and Peninsular Malaysia was flattened (**flatALL**), the mean total rainfall over the west coast on 2 May was higher than in the CTR. The mean total rainfall was less in the inland region than in the CTR because of the absence of orographic rainfall over the Titiwangsa Mountains. Prolonged rain from 1 May to the 2 May during midnight contributed to the higher total rainfall in this experiment.

The final experiment (**noSI**) investigated the role of Sumatra Island. The total daily rainfall over the west coast of Peninsular Malaysia increased significantly. Rainfall along the west coast occurred three times on 2 May. The rainfall over the west coast occurred as early as 03:00 MST on 2 May and stopped after 10:00 MST. Then, another rainfall event occurred at 12:00 MST for almost six hours. At 20:00 MST, another rainfall event occurred near and in the west coast. These events contributed to the high total rainfall in the region. One of the reasons for the frequent rainfalls was the high humidity that is plausible come from the Indian Ocean.

Analysing the control simulation and the other four experiments, the development of the rainfall events on 1 and 2 May can be explained by the following processes as shown in Figure 16:

1. Peninsular Malaysia and Sumatra Island experienced rainfall on the evening of 1 May evening (Figure 16a).

2. The outflows (density currents) from the previous afternoon's rainfall from Sumatra Island and Peninsular Malaysia, along with land breezes enhanced by the anomalously cold air over Sumatra merged into the Strait of Malacca, causing convergence and low-level lifting and triggering the development of convection overnight (Figure 16b).

3. At the same time, a strong northwesterly wind (blue arrow, Figure 16c) from the Indian Ocean brought more moisture and helped to enhance and maintain the convective activity in the Strait of Malacca which then developed into a rainfall cluster on the morning of 2 May that lasted until noon (Figure 16c).

4. By noon of 2 May, another rainfall cluster developed over the Titiwangsa Mountains (Figure 16d).

5. Outflow from the rainfall cluster over the Strait of Malacca, along with a sea breeze, induced convection over the west coast of the peninsula (Figure 16d).

6. The outflow mentioned earlier coming from the west and the outflow from the rainfall over the Titiwangsa Mountains range enhanced the convective activity over the western peninsula (Figure 16d).

7. As the sea breeze circulation strengthened during the day, the rainfall over the strait weakened, and convection over the western peninsula then intensified and produced rainfall (Figure 16e).

8. As the rainfall over the west coast increased, the rainfall over the Titiwangsa Mountains spread to the west and east. The two rainfall clusters along the west coast merged (Figure 16e).

9. The rainfall cluster became stationary on the western peninsula as the Titiwangsa Mountains blocked it from moving eastward despite the prevailing northwesterly wind (Figure 16e).

10. The rainfall cluster continued for a couple of hours and then dissipated.

Overall, both Peninsular Malaysia and the Island of Sumatra are essential in the development of rainfall events over the strait, regardless of the height of the orography. As shown in this case study, orography can play a vital role in enhancing the convection activity over western Peninsular Malaysia. Sumatra Island also plays a crucial role in influencing the local weather of the peninsula. The study has demonstrated that the island of Sumatra has prevented western Peninsular Malaysia from being wetter thus potentially preventing more severe flooding and landslides.

Acknowledgments. The first author is funded by Majlis Amanah Rakyat (MARA) Malaysia, and all authors would like to thank MARA, MetMalaysia (for observational data), NERC (for the UK Met Office Unified Model), NERC staff at the University of Reading, the members of Tropical Hour Met@Reading for input, Stephanie Johnson for the help with the modification of land-mask file for the experiments, Andrew Turner and Geoffrey Wadge for the comments throughout the research and on the thesis, and John Marshall for the comments on the thesis. This work used the ARCHER UK National Supercomputing Service (http://www.archer.ac.uk).

References

Battan, L. J., 1973: *Radar Observation of the Atmosphere*. University of Chicago Press.

Birch, C. E., S. Webster, S. C. Peatman, D. J. Parker, A. J. Matthews, Y. Li, and M. E. E. Hassim, 2016: Scale interactions between the MJO and the western Maritime Continent. *Journal of Climate*, **29 (7)**, 2471–2492, doi:10.1175/JCLI-D-15-0557.1.

Bureau of Meteorology Australia, 2015: Madden-Julian Oscillation (MJO) Index. URL http://www.bom.gov.au/climate/mjo/graphics/rmm.74toRealtime.txt.

Davies, T., M. J. P. Cullen, a. J. Malcolm, M. H. Mawson, a. Staniforth, a. a. White, and N. Wood, 2005: A new dynamical core for the Met Office's global and regional modelling of the atmosphere. *Quarterly Journal of the Royal Meteorological Society*, **131 (608)**, 1759–1782, doi:10.1256/qj.04.101.

Fujita, M., F. Kimura, and M. Yoshizaki, 2010: Morning Precipitation Peak over the Strait of Malacca under a Calm Condition. *Monthly Weather Review*, **138 (4)**, 1474–1486, doi:10.1175/2009MWR3068.1.

Golding, B. W., 1993: A Numerical Investigation of Tropical Island Thunderstorms. *Monthly Weather Review*, **121**, 1417.

Gregory, D., and P. Rowntree, 1990: A Mass Flux Convection Scheme with Representation of Cloud Ensemble Characteristics and Stability-Dependent Closure. *Monthly Weather Review*, **(118)**, 1483.

Holloway, C. E., S. J. Woolnough, and G. M. S. Lister, 2012: Precipitation distributions for explicit versus parametrized convection in a large-domain high-resolution tropical case study. *Quarterly Journal of the Royal Meteorological Society*, **138 (668)**, 1692–1708, doi:10.1002/qj.1903.

Holloway, C. E., S. J. Woolnough, and G. M. S. Lister, 2013: The Effects of Explicit versus Parameterized Convection on the MJO in a Large-Domain High-Resolution Tropical Case Study.

582 Part II: Processes Leading to Differences in MJO Development. *Journal of the Atmospheric*
583 *Sciences*, **72 (7)**, 2719–2743, doi:10.1175/JAS-D-14-0308.1.

584 Huffman, G. J., and D. T. Bolvin, 2007: Real-Time TRMM Multi-Satellite Precipitation Analysis
585 Data Set Documentation. *Laboratory for Atmospheres, NASA Goddard Space Flight Center and*
586 *Science Systems and Applications, Inc*, 26.

587 Joseph, B., B. C. Bhatt, T. Y. Koh, and S. Chen, 2008: Sea breeze simulation over the Malay
588 Peninsula in an intermonsoon period. *Journal of Geophysical Research*, **113**, D20 122, doi:
589 10.1029/2008JD010319.

590 Kamaruzaman, M., M. Adam, and S. Moten, 2012: Rainfall Estimation from Radar Data.
591 *Malaysian Meteorological Department Publication*, **(6)**.

592 Lean, H. W., P. a. Clark, M. Dixon, N. M. Roberts, A. Fitch, R. Forbes, and C. Halliwell, 2008:
593 Characteristics of High-Resolution Versions of the Met Office Unified Model for Forecasting
594 Convection over the United Kingdom. *Monthly Weather Review*, **136**, 3408–3424, doi:10.1175/
595 2008MWR2332.1.

596 Lock, A. P., A. R. Brown, M. R. Bush, G. M. Martin, and R. Smith, 2000: A New Boundary
597 Layer Mixing Scheme . Part I : Scheme Description and Single-Column Model Tests. *Monthly*
598 *Weather Review*, 3187–3199.

599 Love, B. S., A. J. Matthews, and G. M. S. Lister, 2011: The Diurnal Cycle of Precipitation over the
600 Maritime Continent in a High-Resolution Atmospheric Model. *Quarterly Journal of the Royal*
601 *Meteorological Society*, **137 (657)**, 934–947, doi:10.1002/qj.809.

602 Marshall, J. S., and W. M. Palmer, 1948: The size distribution of raindrops. *Quarterly Journal of*
603 *the Royal Meteorological Society*, **76**, 16–36.

MetMalaysia, 2016: General Climate of Malaysia. URL www.met.gov.my/pendidikan/iklim/iklimmalaysia, 1 pp.

NASA, 2019: GIOVANNI v 4.30. URL https://giovanni.gsfc.nasa.gov/giovanni/.

NOAA, 2019: Physical Science Division of Earth System Research Laboratory. URL https://www.esrl.noaa.gov/psd/cgi-bin/db_search/SearchMenus.pl.

Qian, J.-H., 2008: Why Precipitation Is Mostly Concentrated over Islands in the Maritime Continent. *Journal of the Atmospheric Sciences*, **65 (4)**, 1428–1441, doi:10.1175/2007JAS2422.1.

Smith, R. N. B., 2014: A scheme for predicting layer clouds and their water content in a general circulation model. *Quaterly Journal of Royal Meteorological Society*, **128 (5)**, 400–405, doi:10.1017/S0022215114000723.

Sow, K. S., L. Juneng, F. T. Tangang, A. G. Hussin, and M. Mahmud, 2011: Numerical simulation of a severe late afternoon thunderstorm over Peninsular Malaysia. *Atmospheric Research*, **99 (2)**, 248–262, doi:10.1016/j.atmosres.2010.10.014.

Suhaila, J., and A. A. Jemain, 2009: Investigating the impacts of adjoining wet days on the distribution of daily rainfall amounts in Peninsular Malaysia. *Journal of Hydrology*, **368**, 17–25, doi:10.1016/j.jhydrol.2009.01.022.

University of Wyoming, 2016: Atmospheric Soundings - Wyoming Weather Web - University of Wyoming. URL weather.uwyo.edu/upperair/sounding.html.

Wheeler, M. C., and H. H. Hendon, 2004: An All-Season Real-Time Multivariate MJO Index: Development of an Index for Monitoring and Prediction. doi:10.1175/1520-0493(2004)132⟨1917:AARMMI⟩2.0.CO;2.

625 Wilson, D. R., and S. P. Ballard, 1999: A Microphysically based precipitation scheme for the UK
626 Meterological Office Unified Model. *Quarterly Journal of the Royal Meteorological Society*,
627 **125**, 1607–1636.

LIST OF FIGURES

Fig. 1. The location of Peninsular Malaysia and Sumatra. The red circle over the central west coast of the Peninsular Malaysia is known as Klang Valley region. The Klang valley area covers an area of approximately in between 2.6°N to 3.4°N and from the coast line of the western peninsula to 102°E where the Titiwangsa mountains located. The shades represent the orography height. 32

Fig. 2. Rainfall recorded by raingauge in Petaling Jaya station of Malaysian Meteorological Department located shown in Figure 1 for (a) hourly (b) accumulated rainfall. (c) Monthly mean of precipitation of 3 regions (shown in Figure 4) from TRMM dataset. The data range are from 1998 to 2013. 33

Fig. 3. Wind speed (vectors) and wind speed anomaly (shaded) of NCEP/NCAR PSD Reanalysis dataset on 2 May 2012. 34

Fig. 4. The domains for the simulation studies. The outer domain is used in the 12-km model simulation. The inner domain is used in the 1.5-km model simulation. The 1.5-km model domain is 0° - 9°N and 94°E - 105°E. The red dash and letters represent regions which were defined to calculate rainfall amount in the control run to be compared to the experiments. NWC: northwest, WC: west, IL: inland and MS: Strait of Malacca. The shades represent the orography height. 35

Fig. 5. The four sensitivity experiments; Flat Peninsular Malaysia orography (**flatPM**) , flat Sumatra Island orography (**flatSI**), flat both Peninsular Malaysia and Sumatra Island orography (**flatALL**), and the Sumatra Island was removed (**noSI**). The shades here represent the orography height in meters. 36

Fig. 6. Precipitation from radar (top) and 1.5-km model (bottom). Images are from 11:00 MST of 2 May 2012 until 16:00 MST 2 May 2012. These times were selected to compare the development of the rainfall event on 2 May in the afternoon. All values are in mm hr^{-1}. Grey lines on land masses in bottom figures indicate orography feature of above 500 meters. . 37

Fig. 7. The 3-hourly precipitation comparison between TRMM (top), and 1.5-km model (bottom). The 3-hourly mean (as calculated in TRMM, but not at the same grid spacing) was compared to the same rainfall scale, in mm hr^{-1}. Using TRMM, we are able to compare data on the previous day between TRMM and model simulation. Black lines on land masses in bottom figures indicate orography feature of above 500 meters. 37

Fig. 8. (a)Time-longitude Hovmöller plot of precipitation from the 1.5-km model, averaged over 3°N to 4°N and, (b)Time-longitude Hovmöller plot of precipitation from TRMM dataset averaged over 3°N to 4°N. The black dash line indicates the beginning time of the event. The lines 96.7°E and 99.5°E represent the west and east coastlines of Sumatra Island respectively. The lines 101.1°E and 103.5°E represent the west and east coastlines of the Peninsular Malaysia respectively. The topography of both landmasses was also averaged over 3°N to 4°N and shown at the bottom panel. The y-axis is time in Malaysian Standard Time (MST). The x-axis is longitude. 38

Fig. 9. Same as in Figure 8 but for wind direction and magnitude (vectors) and speed (shades) from the 1.5-km model at 233 m (hybrid model level). Black horizontal dashed line represent the beginning time of the event. The contour line represents rainfall above 1 mm hr^{-1}. The topography is shown at the bottom panel. The y-axis is time in Malaysian Standard Time (MST). The x-axis is longitude. 39

Fig. 10. Precipitation and 850hPa winds from the 1.5-km model (CTR) showing the possible mechanisms for this event. (a) Afternoon rainfall on the 1 May (labeled A and B) provided extra moisture to the region to produce overnight rainfall over the Strait of Malacca as shown in panel (b). (c) Later, the convection over the strait and the rainfall in the mountains region over the peninsula influenced the development of rainfall events over the west coast as shown in panel (d). Grey lines on land masses indicate orography feature of above 500 meters. . . 40

Fig. 11. Time-longitude Hovmöller plot, averaged over 3°N to 4°N, of (a) near-surface air temperature anomaly (21m hybrid level, shaded) and near-surface wind (13 m hybrid level, vectors) averaged over 3°N to 4°N from the 1.5-km model. The red arrows show cold outflows moving toward the center of Strait of Malacca. The temperature anomaly is the departure from 48-hour mean temperature. (b) near-surface specific humidity (21m hybrid level, shaded). Red arrows indicate the movement of humidity from both land masses toward the strait overnight. Black horizontal dashed lines represent the beginning time of the event. Dotted contour line indicated a 0 °C and 0 kg/kg values, respectively. The y-axis is time in Malaysian Standard Time (MST), 24-hour format. The x-axis is longitude. 41

Fig. 12. Convergence/divergence plot in the morning of 2 May 2019 from the model simulation showing where the converging winds were likely to occur. Red-brown color represent converging winds and blue color represent diverging winds. Dashed black line represent rainfall above 1 mm hr^{-1}. Green arrows represent winds. All at 13.3 meter model level. Lower right figure shows the plot area. 42

Fig. 13. Precipitation and 850hPa winds for comparison between control run, flat Peninsular Malaysia (**flatPM**), flat Sumatra (**flatSI**), flat Peninsular Malaysia and Sumatra (**flatALL**), and no Sumatra (**noSI**) experiments. The figure compares the main mechanisms in the development of the rainfall on 2 May, in Figure 10. Grey lines on land masses with no orography modification indicate orography feature of above 500 meters. 43

Fig. 14. Same as in Figure 8a and 9 but for all of the experiments. (a,c,e,g,i) precipitation averaged over 3°N to 4°N. (b) 233 m wind (vectors) and wind speed (shaded) averaged over 3°N to 4°N. (d,f,h,j) Same as in (b) but colors represent the wind speed difference from the control run. The same color bar scale is used for both wind speed and wind speed difference. An additional contour line represents the rainfall above 1 mm hr^{-1} was added to the figure. Horizontal black dashed lines indicate the beginning of the event. Panel a and b are for reference only. The y-axis is time in Malaysian Standard Time (MST), 24-hour format. The x-axis is longitude. 44

Fig. 15. Daily precipitation totals for the three regions of interest: (a) northwest coast, NWC, (b) west coast, WC and (c) inland, IL. (d) The central region of the Strait of Malacca, MS, and (e) the location of each region. 45

Fig. 16. (left column) Key mechanisms involved in the development of the severe rainfall event over the west coast of Peninsular Malaysia starting from 1 May and on 2 May. The time is in local standard time and a close estimation of when the mechanisms start to occur. (right column) Key findings on the key mechanism in all experiments. (Illustrated by the first author.) . . . 46

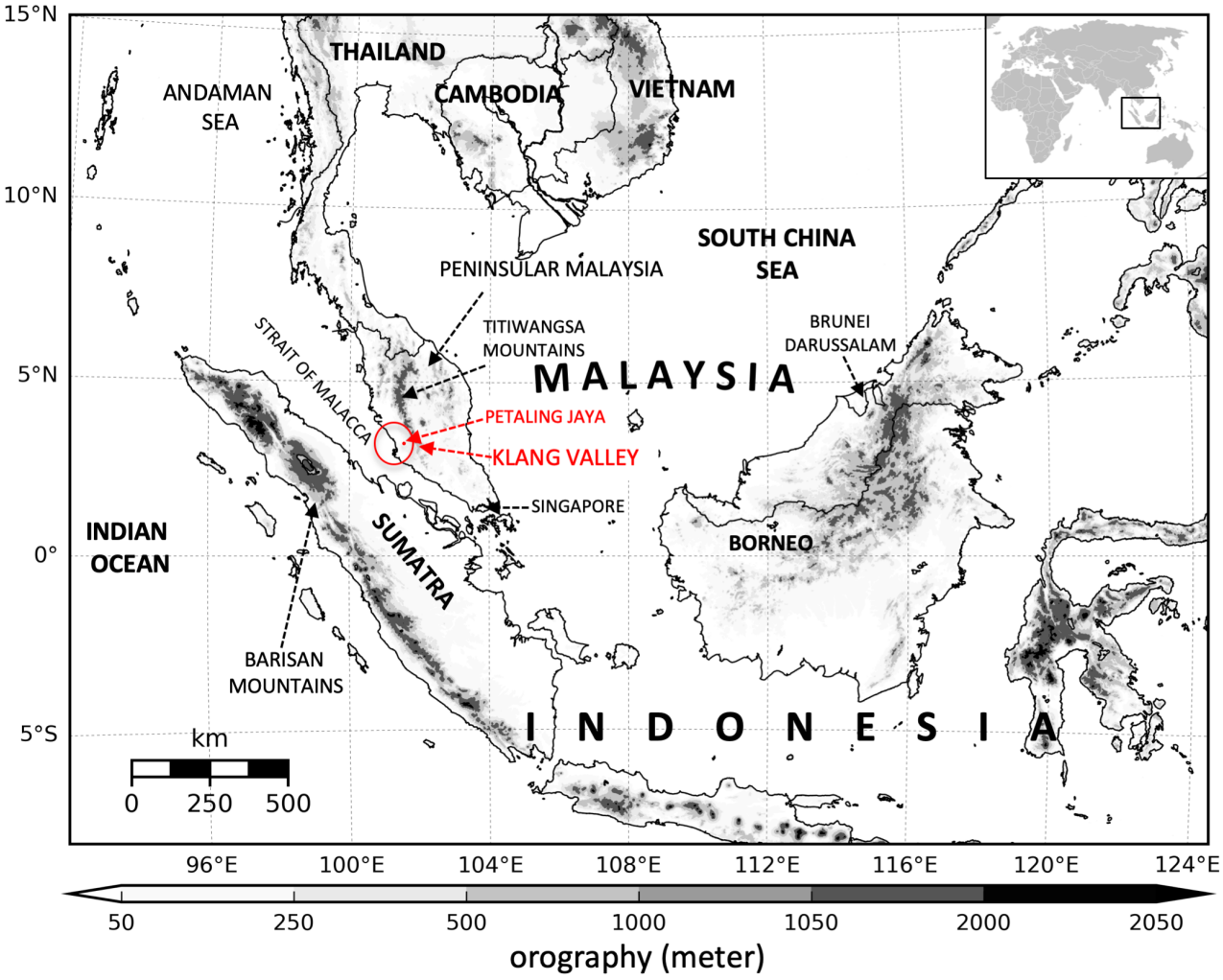

712 FIG. 1. The location of Peninsular Malaysia and Sumatra. The red circle over the central west coast of the
713 Peninsular Malaysia is known as Klang Valley region. The Klang valley area covers an area of approximately
714 in between 2.6°N to 3.4°N and from the coast line of the western peninsula to 102°E where the Titiwangsa
715 mountains located. The shades represent the orography height.

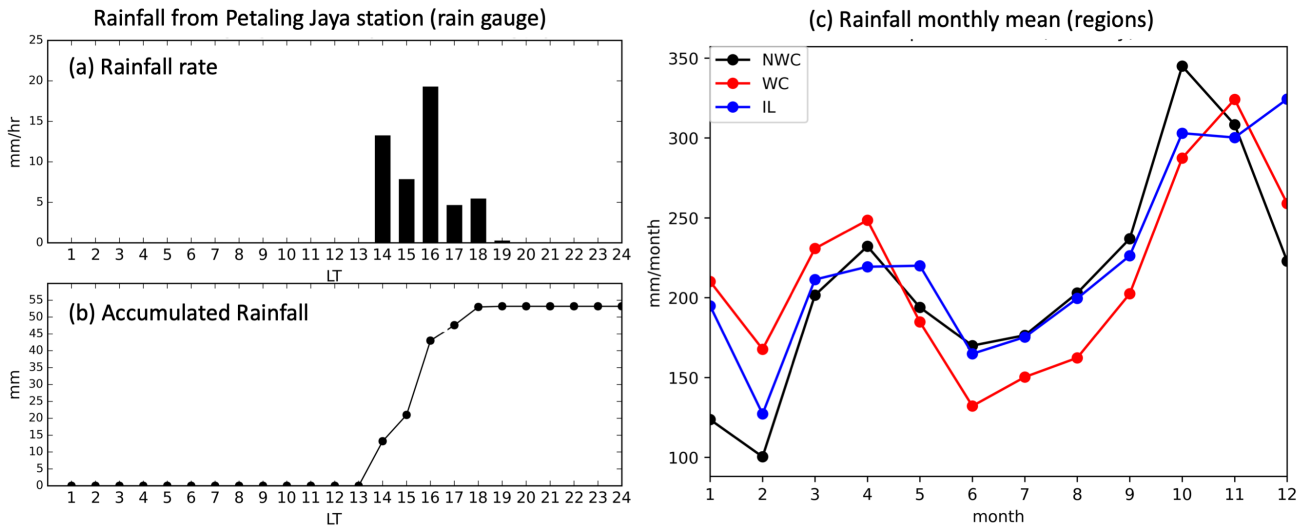

716 FIG. 2. Rainfall recorded by raingauge in Petaling Jaya station of Malaysian Meteorological Department
717 located shown in Figure 1 for (a) hourly (b) accumulated rainfall. (c) Monthly mean of precipitation of 3 regions
718 (shown in Figure 4) from TRMM dataset. The data range are from 1998 to 2013.

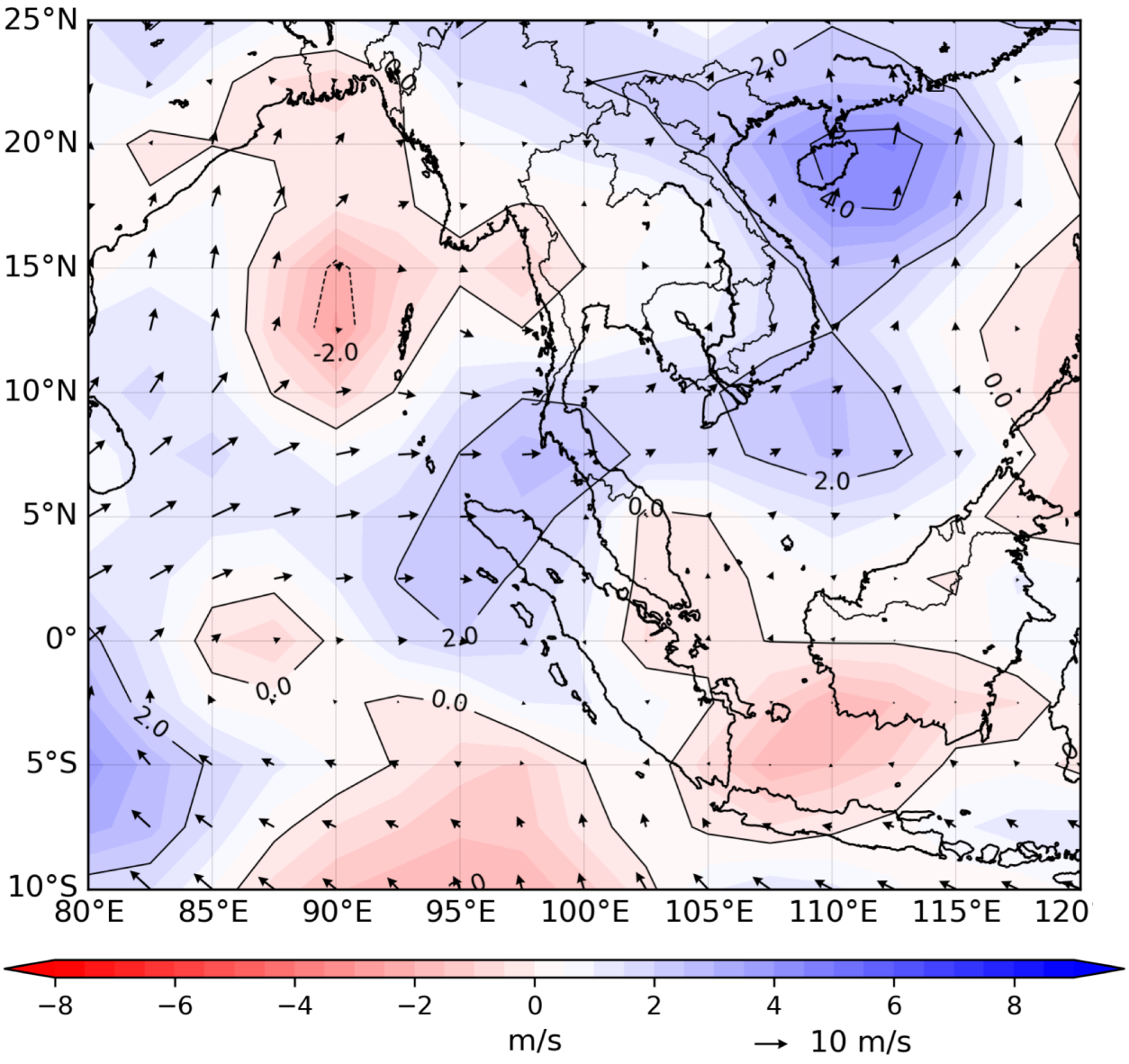

719 FIG. 3. Wind speed (vectors) and wind speed anomaly (shaded) of NCEP/NCAR PSD Reanalysis dataset on
720 2 May 2012.

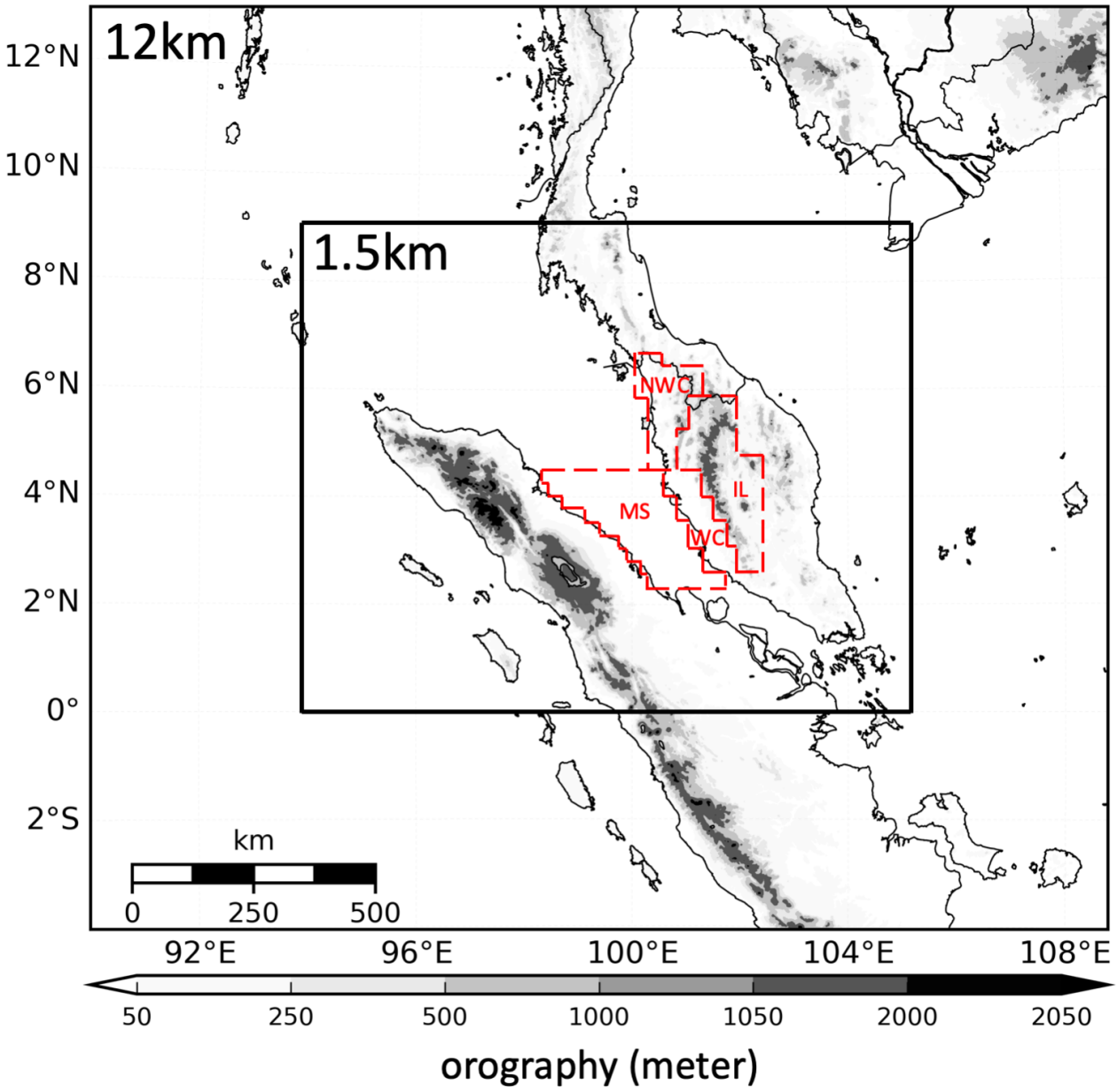

721 FIG. 4. The domains for the simulation studies. The outer domain is used in the 12-km model simulation.
722 The inner domain is used in the 1.5-km model simulation. The 1.5-km model domain is 0° - 9°N and 94°E -
723 105°E. The red dash and letters represent regions which were defined to calculate rainfall amount in the control
724 run to be compared to the experiments. NWC: northwest, WC: west, IL: inland and MS: Strait of Malacca. The
725 shades represent the orography height.

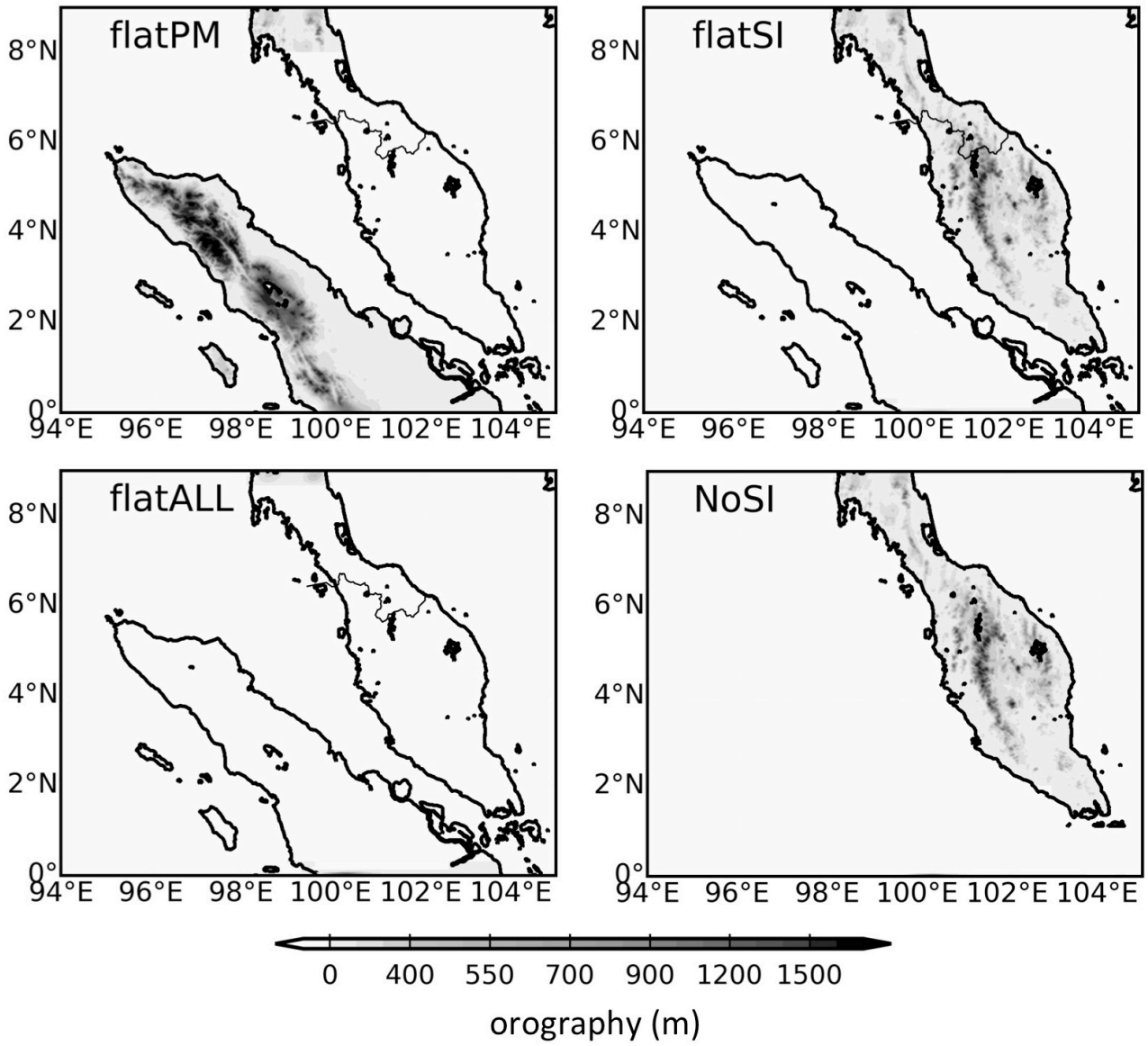

726 FIG. 5. The four sensitivity experiments; Flat Peninsular Malaysia orography (**flatPM**) , flat Sumatra Island
727 orography (**flatSI**), flat both Peninsular Malaysia and Sumatra Island orography (**flatALL**), and the Sumatra
728 Island was removed (**noSI**). The shades here represent the orography height in meters.

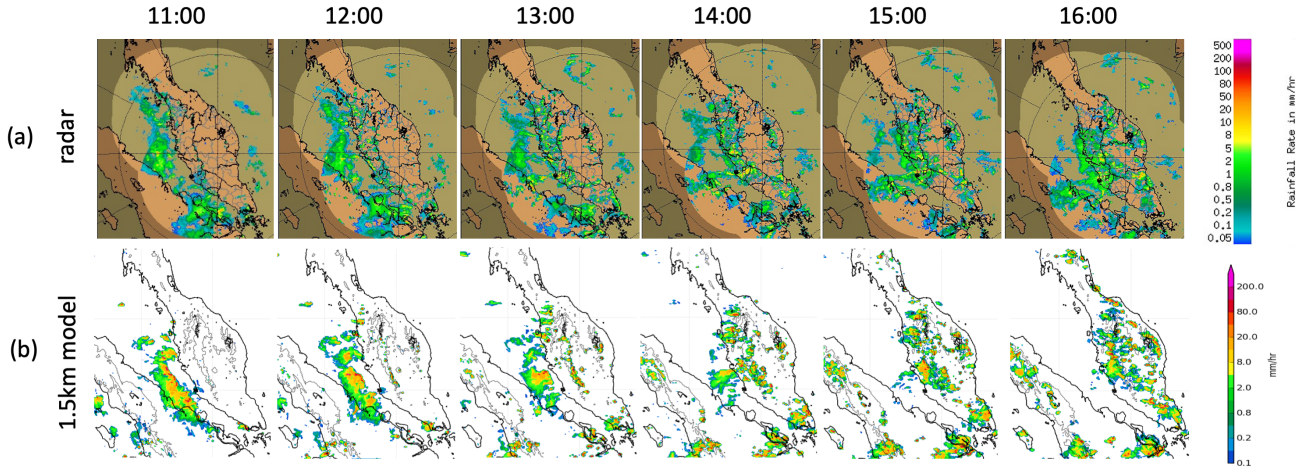

729 FIG. 6. Precipitation from radar (top) and 1.5-km model (bottom). Images are from 11:00 MST of 2 May
730 2012 until 16:00 MST 2 May 2012. These times were selected to compare the development of the rainfall event
731 on 2 May in the afternoon. All values are in mm hr^{-1}. Grey lines on land masses in bottom figures indicate
732 orography feature of above 500 meters.

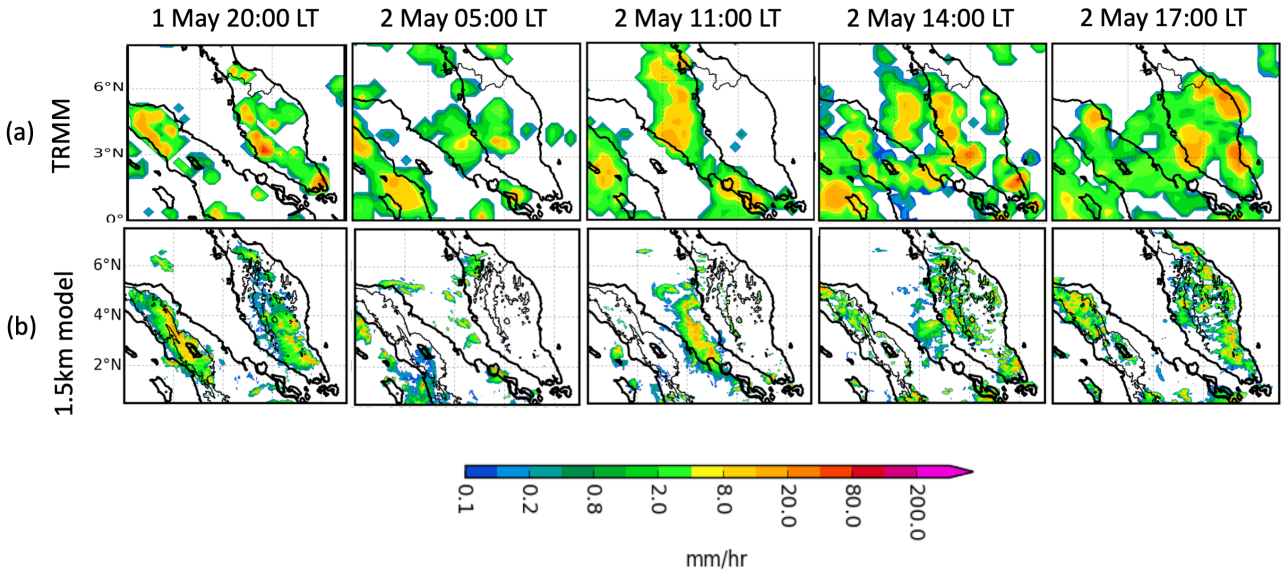

733 FIG. 7. The 3-hourly precipitation comparison between TRMM (top), and 1.5-km model (bottom). The 3-
734 hourly mean (as calculated in TRMM, but not at the same grid spacing) was compared to the same rainfall
735 scale, in mm hr^{-1}. Using TRMM, we are able to compare data on the previous day between TRMM and model
736 simulation. Black lines on land masses in bottom figures indicate orography feature of above 500 meters.

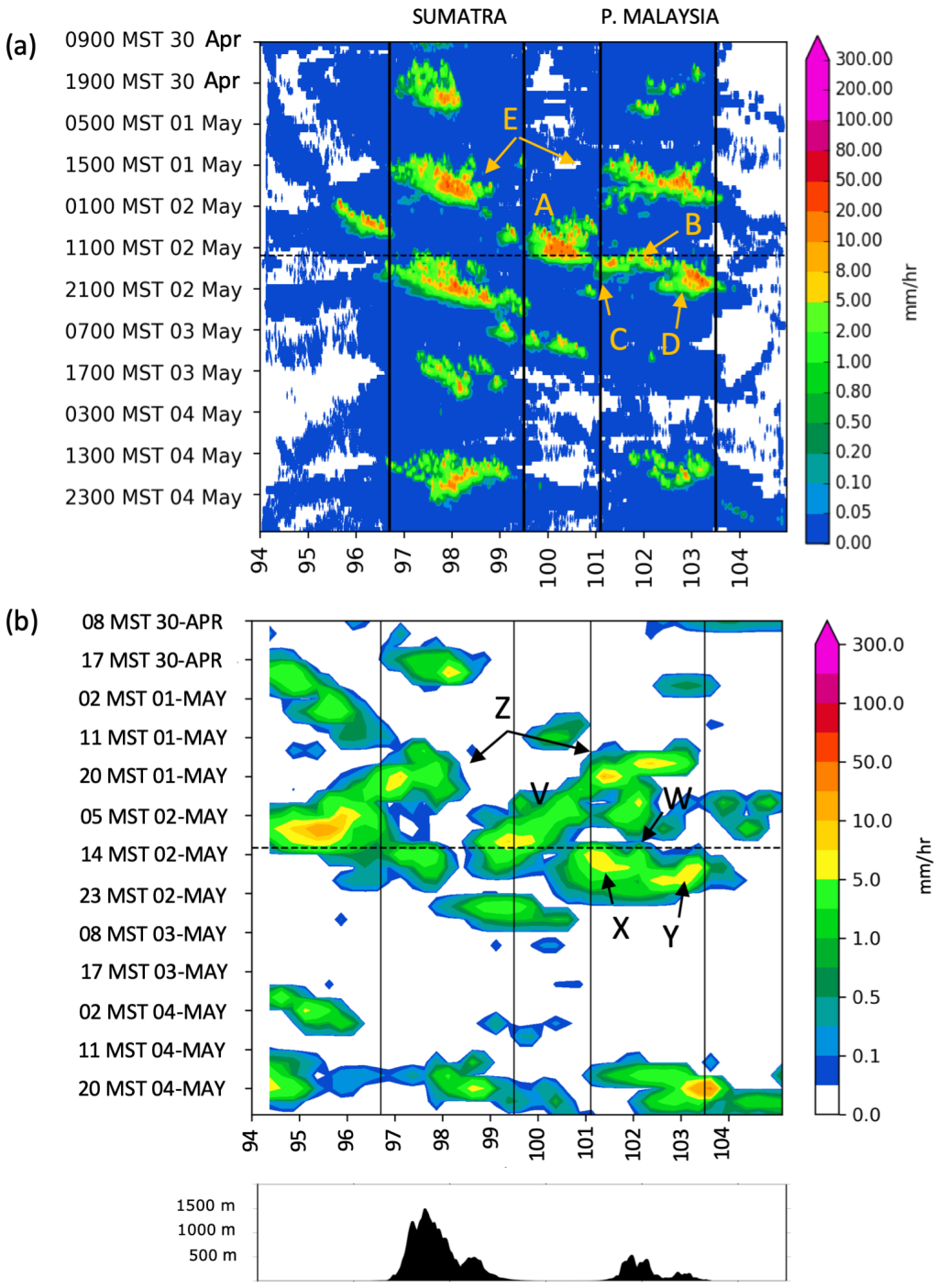

737 FIG. 8. (a)Time-longitude Hovmöller plot of precipitation from the 1.5-km model, averaged over 3°N to
738 4°N and, (b)Time-longitude Hovmöller plot of precipitation from TRMM dataset averaged over 3°N to 4°N.
739 The black dash line indicates the beginning time of the event. The lines 96.7°E and 99.5°E represent the west
740 and east coastlines of Sumatra Island respectively. The lines 101.1°E and 103.5°E represent the west and east
741 coastlines of the Peninsular Malaysia respectively. The topography of both landmasses was also averaged over
742 3°N to 4°N and shown at the bottom panel. The y-axis is time in Malaysian Standard Time (MST). The x-axis
743 is longitude.

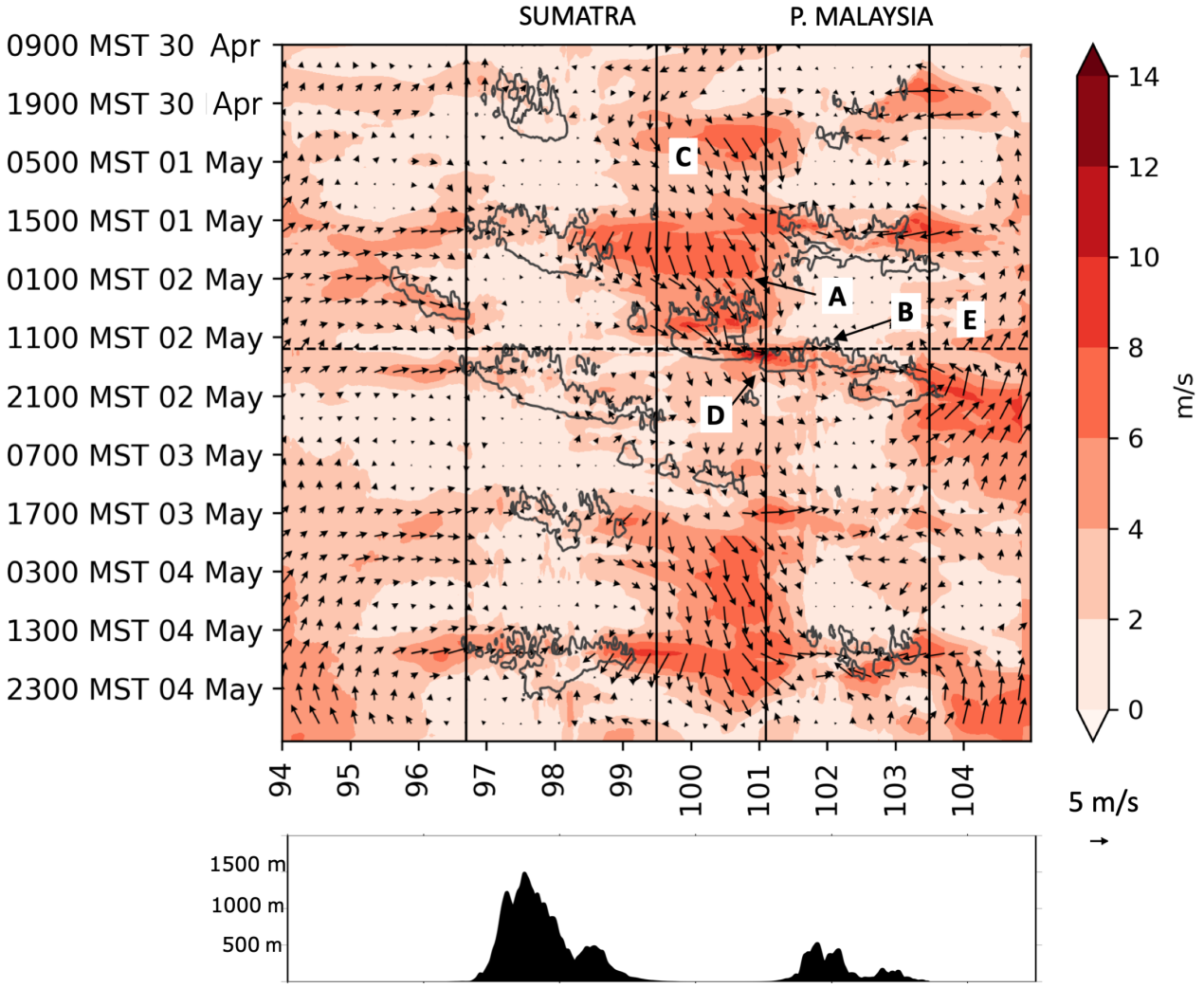

744 FIG. 9. Same as in Figure 8 but for wind direction and magnitude (vectors) and speed (shades) from the
745 1.5-km model at 233 m (hybrid model level). Black horizontal dashed line represent the beginning time of the
746 event. The contour line represents rainfall above 1 mm hr^{-1}. The topography is shown at the bottom panel. The
747 y-axis is time in Malaysian Standard Time (MST). The x-axis is longitude.

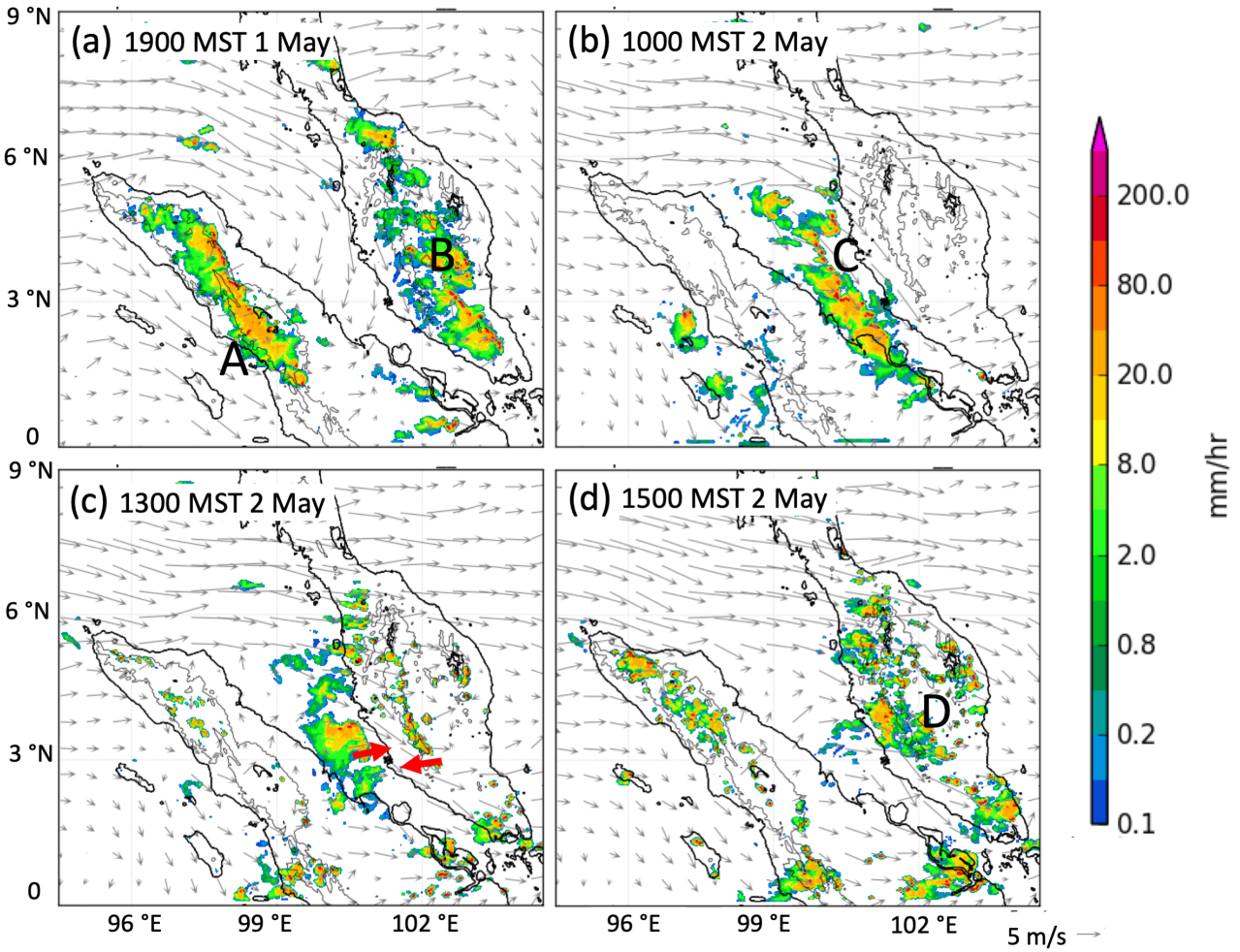

748 FIG. 10. Precipitation and 850hPa winds from the 1.5-km model (CTR) showing the possible mechanisms
749 for this event. (a) Afternoon rainfall on the 1 May (labeled A and B) provided extra moisture to the region to
750 produce overnight rainfall over the Strait of Malacca as shown in panel (b). (c) Later, the convection over the
751 strait and the rainfall in the mountains region over the peninsula influenced the development of rainfall events
752 over the west coast as shown in panel (d). Grey lines on land masses indicate orography feature of above 500
753 meters.

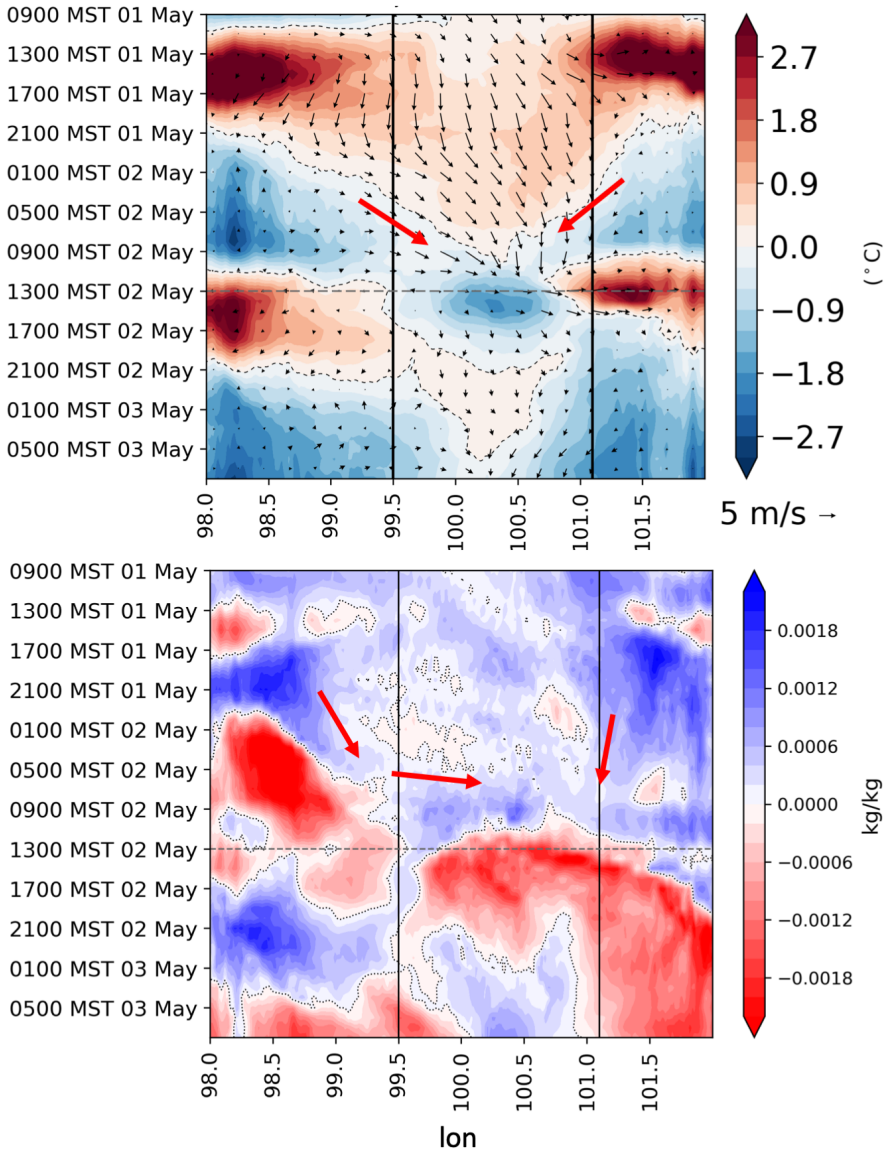

754 FIG. 11. Time-longitude Hovmöller plot, averaged over 3°N to 4°N, of (a) near-surface air temperature
755 anomaly (21m hybrid level, shaded) and near-surface wind (13 m hybrid level, vectors) averaged over 3°N to
756 4°N from the 1.5-km model. The red arrows show cold outflows moving toward the center of Strait of Malacca.
757 The temperature anomaly is the departure from 48-hour mean temperature. (b) near-surface specific humidity
758 (21m hybrid level, shaded). Red arrows indicate the movement of humidity from both land masses toward the
759 strait overnight. Black horizontal dashed lines represent the beginning time of the event. Dotted contour line
760 indicated a 0 °C and 0 kg/kg values, respectively. The y-axis is time in Malaysian Standard Time (MST), 24-hour
761 format. The x-axis is longitude.

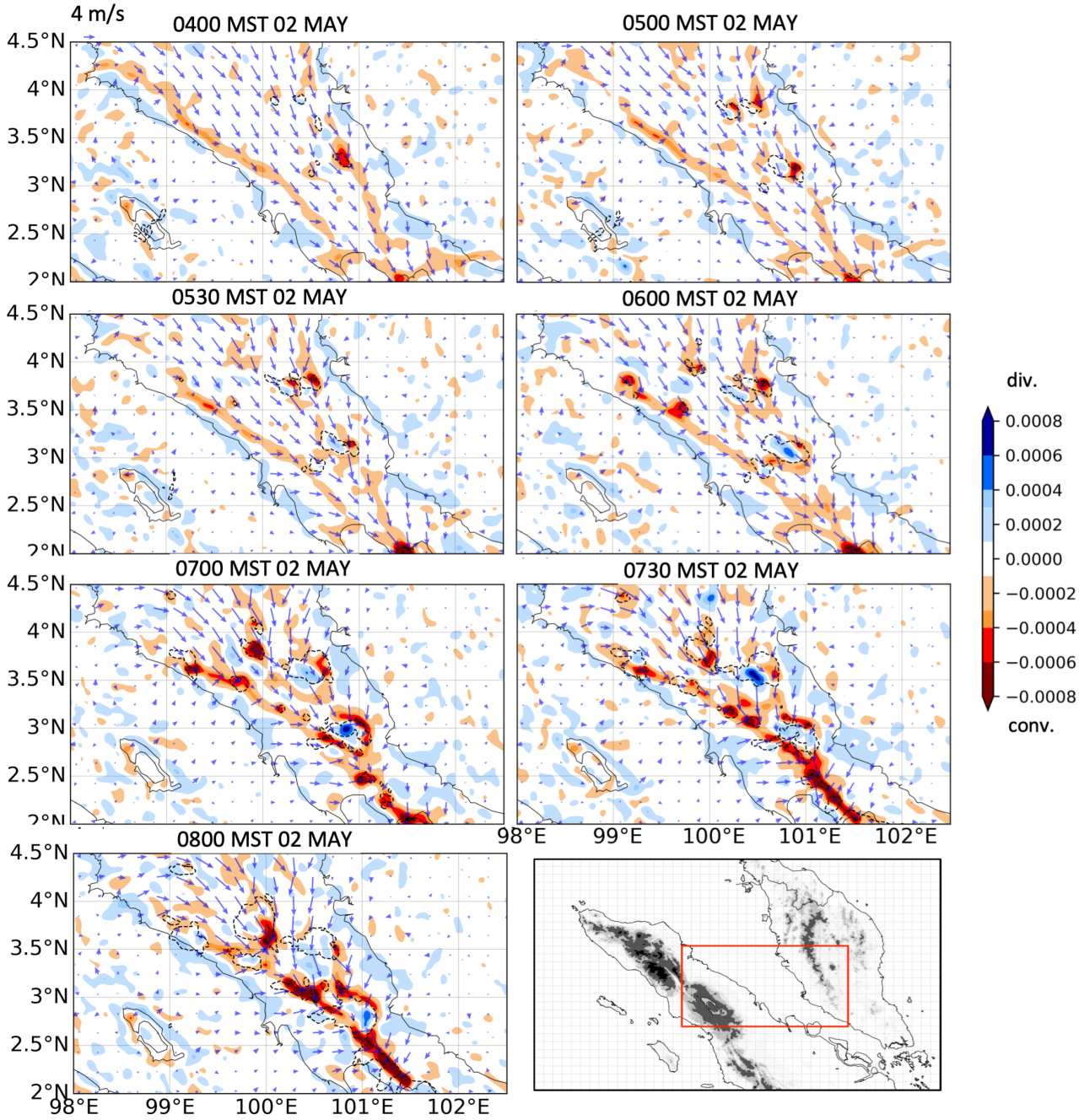

762 FIG. 12. Convergence/divergence plot in the morning of 2 May 2019 from the model simulation showing
763 where the converging winds were likely to occur. Red-brown color represent converging winds and blue color
764 represent diverging winds. Dashed black line represent rainfall above 1 mm hr^{-1}. Green arrows represent winds.
765 All at 13.3 meter model level. Lower right figure shows the plot area.

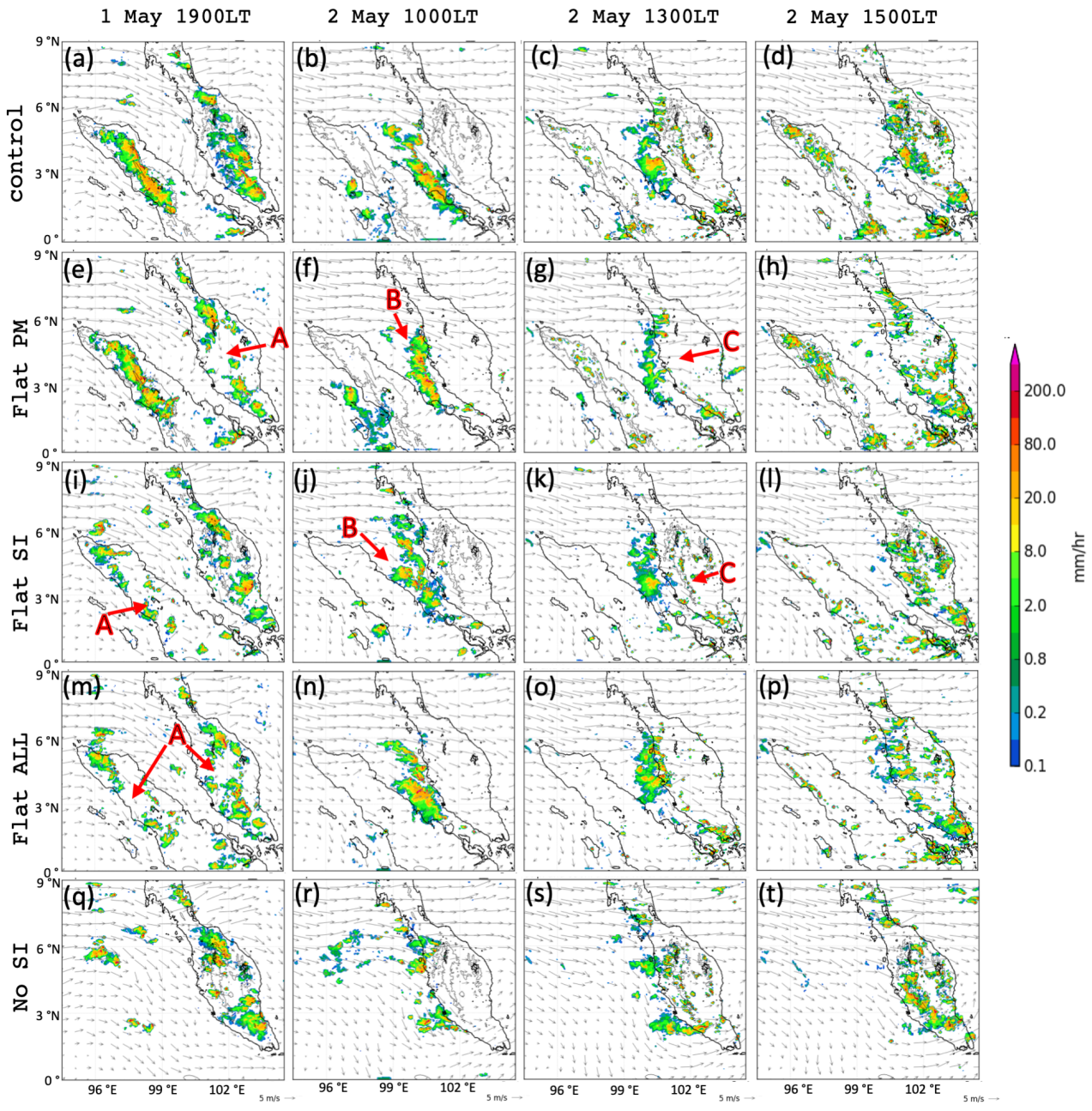

766 FIG. 13. Precipitation and 850hPa winds for comparison between control run, flat Peninsular Malaysia
767 (**flatPM**), flat Sumatra (**flatSI**), flat Peninsular Malaysia and Sumatra (**flatALL**), and no Sumatra (**noSI**) ex-
768 periments. The figure compares the main mechanisms in the development of the rainfall on 2 May, in Figure 10.
769 Grey lines on land masses with no orography modification indicate orography feature of above 500 meters.

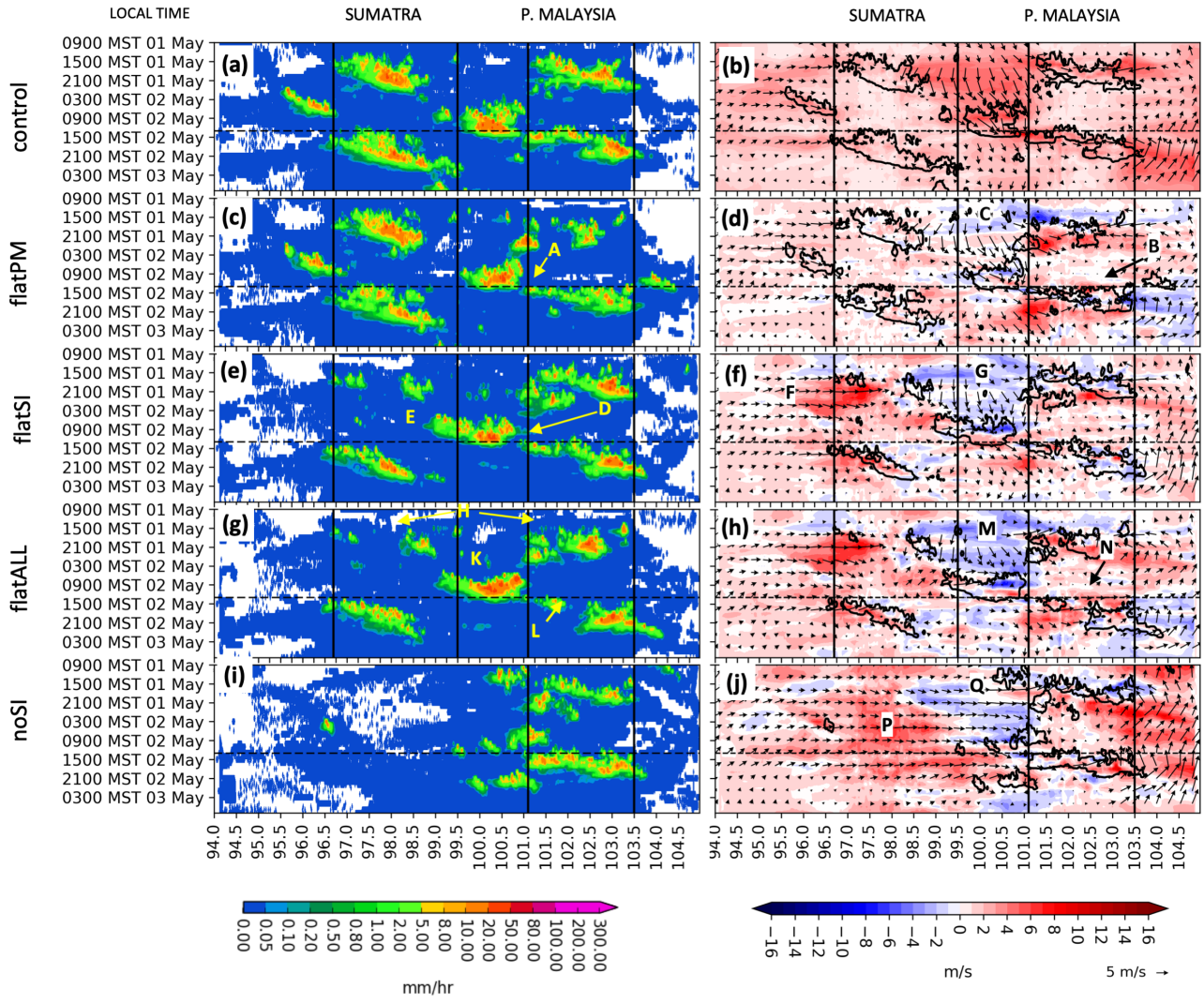

770 FIG. 14. Same as in Figure 8a and 9 but for all of the experiments. (a,c,e,g,i) precipitation averaged over 3°N
771 to 4°N. (b) 233 m wind (vectors) and wind speed (shaded) averaged over 3°N to 4°N. (d,f,h,j) Same as in (b) but
772 colors represent the wind speed difference from the control run. The same color bar scale is used for both wind
773 speed and wind speed difference. An additional contour line represents the rainfall above 1 mm hr^{-1} was added
774 to the figure. Horizontal black dashed lines indicate the beginning of the event. Panel a and b are for reference
775 only. The y-axis is time in Malaysian Standard Time (MST), 24-hour format. The x-axis is longitude.

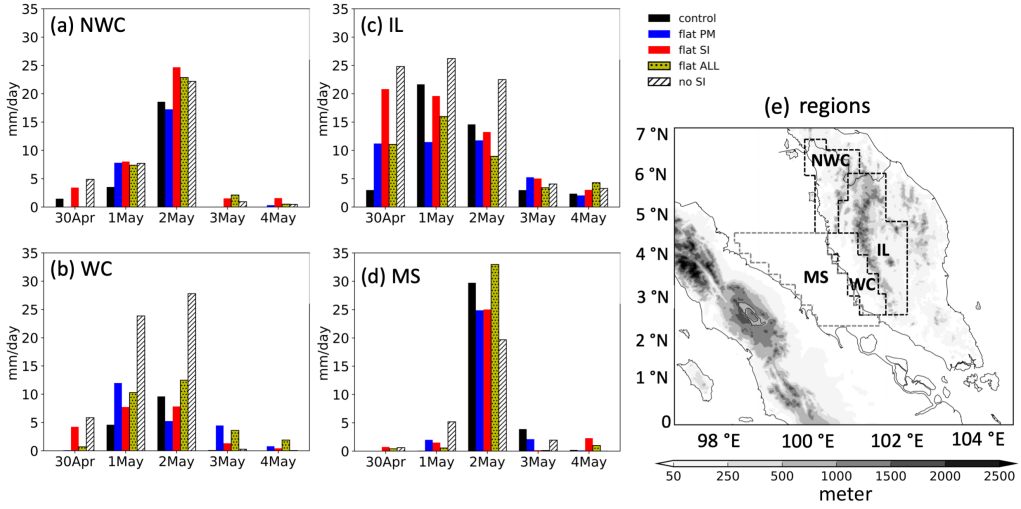

776 FIG. 15. Daily precipitation totals for the three regions of interest: (a) northwest coast, NWC, (b) west coast,
777 WC and (c) inland, IL. (d) The central region of the Strait of Malacca, MS, and (e) the location of each region.

Mechanisms	Key findings
(a) 2000 MST 1 May 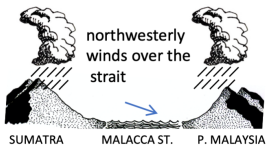	i). Both Sumatra and Peninsular Malaysia experienced late afternoon rainfall in the 1 May. ii). Rainfall in 1 May evening occurred in **all models run**.
(b) 0000 MST 2 May 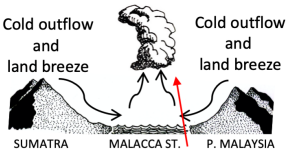 Convection developed due to cold flow + land breezes and northwesterly winds convergence	i). Cold outflows as a product of the evening rainfall flow toward the Strait of Malacca from both land masses by midnight, in all runs **except NoSI.**
(c) 0500 MST 2 May 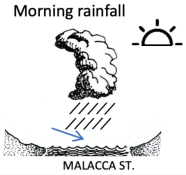	i). Morning rainfall occurred on 2 May in **control**, **flat PM**, **flat SI**, and **flat ALL** runs. ii). Morning rainfall in **NoSI** experiment concentrated closer to the peninsula coast.
(d) 1400 MST 2 May 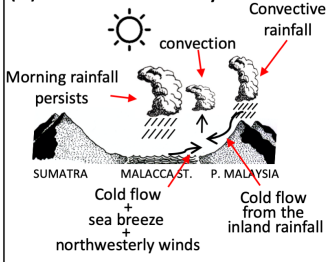	i). In **control** and **flat SI** runs: Convection over the western peninsula influenced by rainfall over the strait and sea breeze mechanism, as well as the rainfall over the peninsular from insolation and orographic lifting. ii). In **flatPM** and **flatALL** runs: Convection over the western coast influenced by morning rainfall over the strait and sea breeze mechanism over the peninsula (insolation). iii). In **NoSI** run: convection developed from both convection due to insolation and orographic lifting with possible moister westerly wind.
(e) 1500 MST 2 May 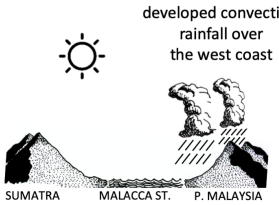	i). In **control**, **flatSI**, **NoSI** runs: developed rainfall system stay on the west longer as the mountains prevent it to move eastward. ii). In **flatPM** and **flatALL** runs: rainfall system moved eastward following the prevailing westerly winds as there are no mountains to prevent.

FIG. 16. (left column) Key mechanisms involved in the development of the severe rainfall event over the west coast of Peninsular Malaysia starting from 1 May and on 2 May. The time is in local standard time and a close estimation of when the mechanisms start to occur. (right column) Key findings on the key mechanism in all experiments. (Illustrated by the first author.)